Earth and Planetary Science
https://journals.nasspublishing.com/index.php/eps

ARTICLE

Surface and Subsurface Mapping of the Duchesne Fault Zone, Utah, USA

Alan Ketring , ***John McBride*** * , ***A. Riley Brinkerhoff*** , ***Ronald A. Harris*** , ***Samuel M. Hudson*** , ***Kevin A. Rey***

Department of Geological Sciences, Brigham Young University, Provo, UT 84602, USA

ABSTRACT

The Duchesne Fault Zone (DFZ) consists of a series of east-west trending *en echelon* opening mode fractures in the Uinta Basin, eastern Utah (USA), which developed synchronously above the neutral surface of the Duchesne Anticline during the Laramide Orogeny. The Duchesne Graben (DG) was formed by decreasing displacement towards the neutral surface. Lake Canyon, an area exposing the subsurface geology on the western part of the DFZ, serves as an analogue for fold formation within the saline facies of the lower Green River Formation, while Indian Canyon, an area created by dip-slip faulting of the DG, exposes faulting within the sandstone-limestone facies of the lower Green River Formation. The two canyons illustrate different stress regimes during the formation of these structures influenced by the Laramide orogeny. The presence of an anticlinal fold within Indian Canyon, together with the overlying DG, indicates the coexistence of opposing stress regimes within the DFZ that accommodate space problems caused by contractional deformation at depth. Extension, above the folding as mapped in the DG, dominates the upper portions of a large anticlinal fold above the neutral surface. In this way, the DFZ acted as a hinge point in the developing Uinta Basin, with steeper stratigraphic dips to the north of the fault zone. Our results imply petroleum reservoir behaviour along the DFZ is influenced by opposing stress regimes that created faults that act both as conduits for increased permeability and as seals for reservoir compartmentalisation.

Keywords: Uinta Basin; Duchesne Fault Zone; Geological Structure

*CORRESPONDING AUTHOR:
John McBride, Department of Geological Sciences, Brigham Young University, Provo, UT 84602, USA; Email: john_mcbride@byu.edu

ARTICLE INFO
Received: 6 January 2026 | Revised: 2 March 2026 | Accepted: 13 March 2026 | Published Online: 25 March 2026
DOI: https://doi.org/10.36956/eps.v5i1.3063

CITATION
Ketring, A., McBride, J., Brinkerhoff, A.R., et al., 2026. Surface and Subsurface Mapping of the Duchesne Fault Zone, Utah, USA. Earth and Planetary Science. 5(1): 20–46. DOI: https://doi.org/10.36956/eps.v5i1.3063

1. Introduction

The Duchesne Fault Zone (DFZ) is a major structure in the Uinta Basin of northeastern Utah, roughly paralleling the south flank of the Uinta Mountains (**Figure 1**)[1–4]. It is composed of an east-west-trending system of normal faults located in the northern portion of the Uinta Basin. It extends for approximately 40 to 70 km south of the Uinta Basin axis and north of the basin's topographic low (**Figure 1**). The DFZ is part of the larger structural framework of the Uinta Basin, a deep, asymmetric basin formed during the Laramide Orogeny. In this study, based on our surface and subsurface mapping, we will describe the surface features as the Duchesne Graben and the whole system as the Duchesne Fault Zone (DFZ). The fault zone is expressed as a distinct linear topographic escarpment, in some places up to 6 m high, cutting across the relatively flat terrain of the basin (**Figure 1**)[3,5–9]. As can be seen from satellite images and digital elevation models (**Figure 2a–d**), the DFZ is characterised by a complex array of segmented structures, instead of a single continuous fault. Its structural style consists primarily of an *en echelon* system of high-angle normal faults, forming a series of horsts and grabens. Subsurface stratigraphic throw across the faults ranges from a few meters to 150–200 m[5,6]. The faults on the south side of the grabens typically are the master faults, with antithetic faults on the north side (**Figure 3** and **Table 1**). The stratigraphic relationship to faulting indicates post-Eocene activity. The eastern portion of the DFZ primarily displaces the Eocene Uinta Formation (**Figure 4a,b**), while along the western portion, faults cut the Eocene-Oligocene Duchesne River Formation (**Figure 4b**)[5,6].

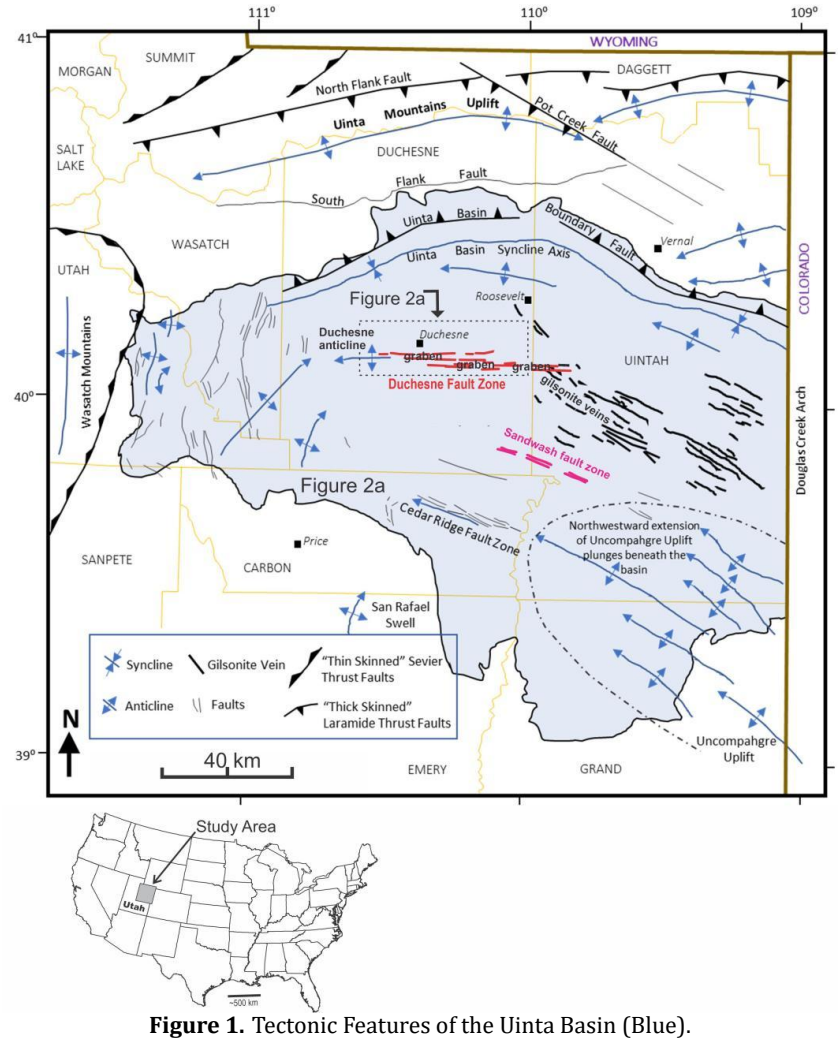

Figure 1. Tectonic Features of the Uinta Basin (Blue).

Source: Modified from Brinkerhoff et al.[7–9]. County boundaries and names are shown.

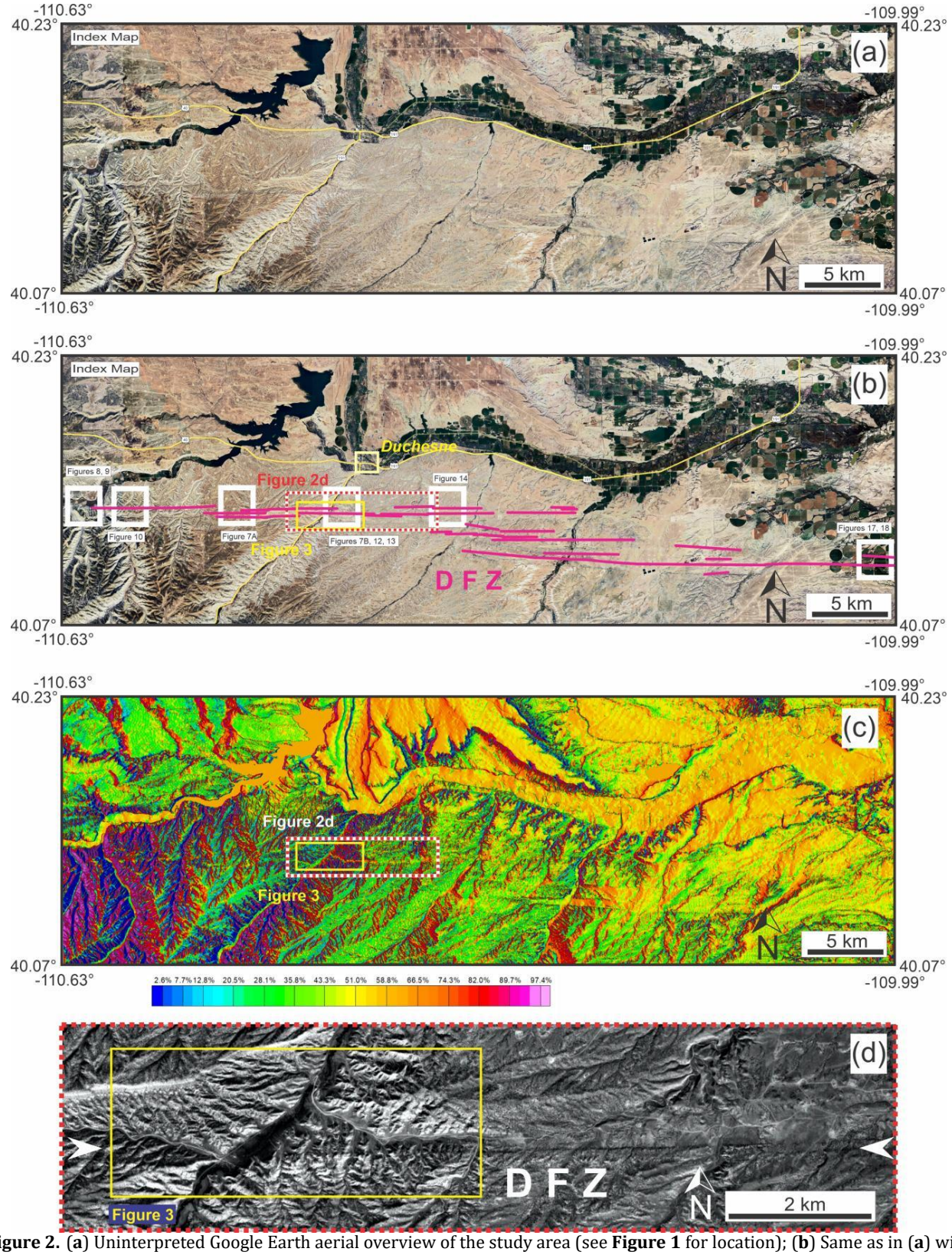

Figure 2. (**a**) Uninterpreted Google Earth aerial overview of the study area (see **Figure 1** for location); (**b**) Same as in (**a**) with annotation; (**c**) Same area as in (**a**), but digital elevation model data processed as illuminated shaded relief; (**d**) Excerpt of grey-level Google Earth image (see **Figure 2b,c** for location).

Note: DFZ in **Figure 2b** is the Duchesne Fault Zone. White squares indicate locations of figures referred to in this study; Rectangles in **Figure 2c** show the locations of figures referred to in this study; The yellow rectangle in **Figure 2d** shows the location of **Figure 3**.

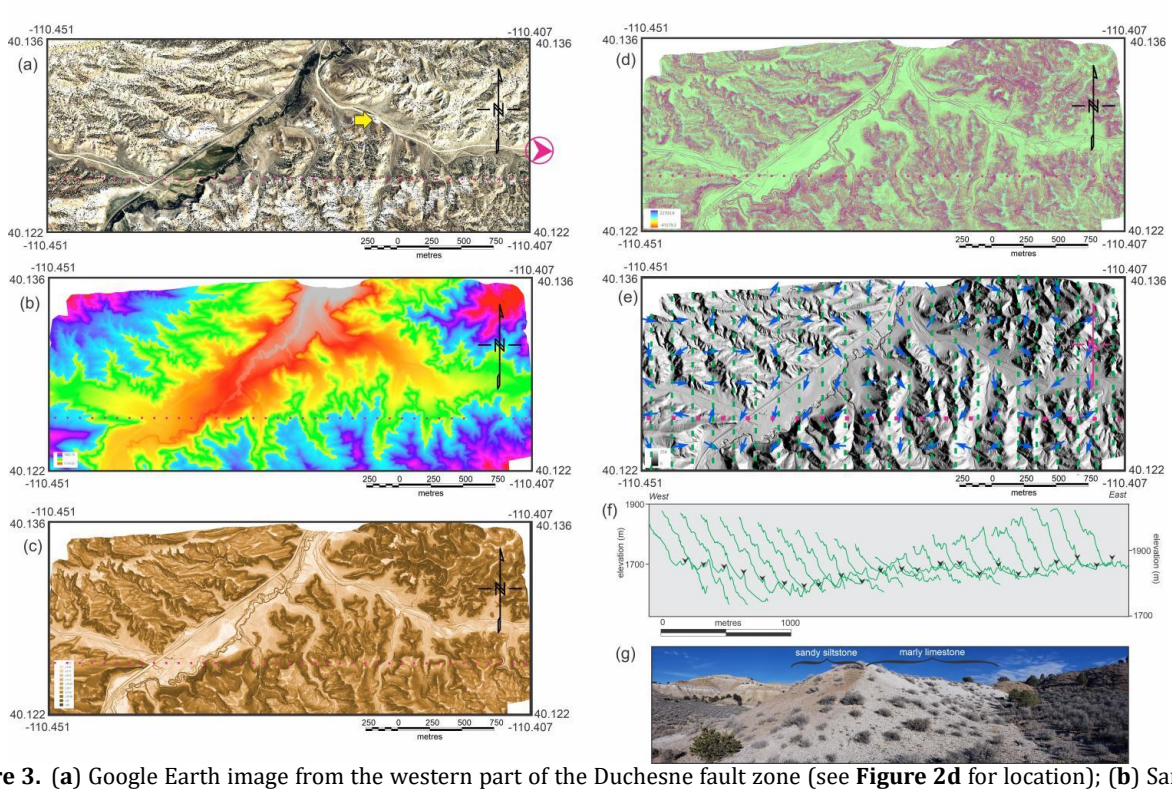

Figure 3. (**a**) Google Earth image from the western part of the Duchesne fault zone (see **Figure 2d** for location); (**b**) Same as **Figure 3a**, but colour raster image from LiDAR survey collected for this study; (**c**) LiDAR processed as elevation slope; (**d**) LiDAR processed as elevation curvature; (**e**) LiDAR processed as elevation shaded relief ("hillshade"); (**f**) North-to-south elevation profiles shown in skew format, spaced about 165 m, extracted from the LiDAR survey (**Figure 3b**); (**g**) Outcrop view along the DFZ (Duchesne Graben), showing the origin of white rock colour seen along the fault trace in **Figure 3a** (red dashed line).
Note: The red-dashed line in **Figure 3a** is the DFZ trace (from **Figure 2d**); The red arrow indicates the location and orientation of the drone image in **Figure 5**; Green dashed lines in **Figure 3e** mark LiDAR elevation profiles in **Figure 3f**; Black arrows in **Figure 3f** are DFZ (from **Figure 2d**); The outcrop (40°7.839′ N, 110°25.325′ W; see yellow arrow in **Figure 3a**) in **Figure 3g** is the Sandstone-limestone Member of the Green River Formation, looking to the east.

Table 1. Comparison of DFZ Fault Geometries: West vs. East.

Fault Style	West	East
Characteristics	Well-developed, forming a symmetric graben	Less continuous: often expressed as a series of small "step-down" faults
Vertical throw	Higher, often exceeding 100 m at the surface	Lower, typically 15–45 m, dissipating rapidly.

Sources: Groeger and Bruhn [3], Brinkerhoff and Sprinkel [4], and Utah Geological Survey [6].

Understanding the subsurface structure of petroleum-rich areas is vital for effective exploration, especially in regions with complex faulting, such as around the Duchesne Fault Zone (DFZ) of the Uinta Basin, eastern Utah, USA (**Figure 1**) [1,9]. The DFZ is closely tied to the region's concentrated oil and gas production by facilitating hydrocarbon extraction due to increased fracturing along the zone. To gain a better understanding of the geometry of the underlying geology and its impact on petroleum production, multiple methods were employed to reconstruct the geological history. These include geometric analyses using stereographic projections of bedding and fault planes, cross-sections, photogrammetry models, and digital elevation data. The combination of these methods helps to uncover the structural history of the lower Green River Formation (**Figure 4**) within the DFZ. This formation is especially significant because it is one of the largest oil-producing reservoirs in Utah [7].

Previous studies proposed two competing structural models for the fault's depth: a "detachment model" where the fault flattens into a bedding plane at roughly 930 m depth, and a "planar model" [3] where displacement decreases with depth, dying out around 1,365 m. Groeger and Bruhn [3] favoured the planar model based on comparisons with nearby fault systems. While

predominantly extensional (dip-slip), researchers have noted evidence of strike-slip and oblique motion. Utah Geological Survey[6] described the fault as a "hingeline" feature, antithetic to the major boundary faults of the Uinta Basin, with as much as 200 m of slip on the master fault. Smith[10] investigated the intense fracturing within the zone, concluding that high fluid pressures played a critical role in fracture initiation and propagation, distinguishing the DFZ from other local flexures that lack such intense fracturing. Although conflicting interpretations exist as to Quaternary movement along the DFZ[5,11,12], the current consensus is that no detailed palaeoseismic investigations (such as trenching) have confirmed significant Quaternary movement[2].

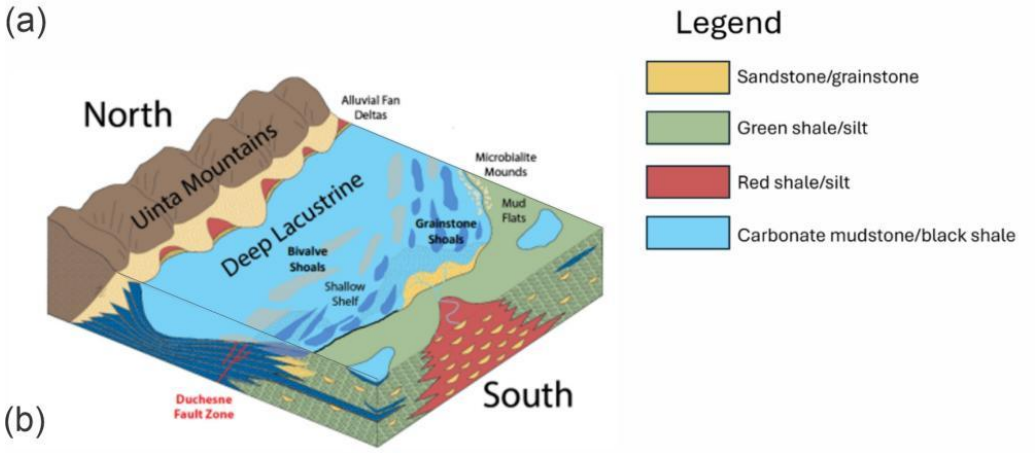

SYMBOL	SYMBOL		THICKNESS (METERS)	Lithology (NOT TO SCALE)
Tuc	Uinta Form.	member C	570-650	
Tub		member B	35-665	
Tgsl	Green River Formation	sandstone and limestone facies	as much as 300	
Tgss		sandstone facies	0-275	
Tgs		saline facies	as much as 350	Oily tuff
Tgpu		upper Parachute Creek Member	200-400	
Tgpl		lower Parachute Creek Member (Garden Gulch Member)	570-680	Mahogany oil-shale marker bed

Figure 4. (**a**) Depositional model of the rock types within the Green River Formation. Note the location of the DFZ within the lake; (**b**) Stratigraphic column of Green River Formation lithologies that formed within ancient Lake Uinta.

2. Regional Geology

Late Cretaceous to Paleogene contraction during the Laramide Orogeny caused inversion of the Uinta Basin. This crustal thickening process caused reactivation of pre-existing normal faults—originally formed by extension—as reverse faults. Crustal thickening loaded the adjacent lithosphere, inducing a flexural response in the basin south of the Laramide thrust front[1–5]. Movement on the DFZ was recurrent throughout the long ex-

panse of Green River sedimentation. This event gave rise to the east-west-trending Uinta Basin. The northern edge of the basin is bordered by the Uinta Mountains, while on the south, it is flanked by the northwest-plunging Uncompahgre Uplift and the north-plunging San Rafael Swell. To the east of the Duchesne Fault Zone lies the north-plunging Douglas Creek Arc, and the western boundary is marked by the north-south trending Wasatch Fault, part of the Basin and Range region.

The Sevier and Laramide Orogenies were instrumental in forming the Uinta Basin during the Jurassic to early Cenozoic era by generating thickened crust through horizontal shortening, leading to uplift and peripheral subsidence [6–9]. During the transition from the Maastrichtian to the late Palaeocene—from the Sevier to the Laramide orogenies—flexural down-warping caused by the weight of surrounding mountains created transitional sedimentary basins in what are now the southern, western, and central regions of the Uinta Basin. By the early Eocene, several freshwater lakes had developed in the basin [7]. These lakes expanded as a result of subsidence during the Long Point Transgression, which shifted the basin from an open hydrological system to a closed one, converting ancient Lake Uinta from a freshwater to a saline lake (**Figure 4a,b**).

The transgression of ancestral Lake Uinta and the simultaneous subsidence of the Uinta Basin resulted in the deposition of lacustrine sediments. In the northern region, these sediments originate from erosion of the rising Uinta Mountains, while in the south, they source from uplift of the San Rafael Swell and the Uncompahgre Range [13,14] (**Figure 1**). This sediment deposition led to the formation of the Green River, Wasatch, and Colton formations, all of which contain hydrocarbons [15]. The sedimentary rocks within the DFZ include Eocene-aged sandstone, shale, and lacustrine limestone from the Lower Green River and Uinta formations, serving as useful markers on gamma-ray well logs [3]. The most common surface facies within the lower Green River and Uinta formations are the sandstone-limestone facies, the saline facies, and Member B, all of which have been informally named in previous studies [16] (**Figure 3**). During the Cretaceous and early Tertiary periods, rising lake levels led to deposition of various shallow water carbonate rocks. These carbonate markers are valuable for correlating offshore lacustrine rocks with marginal lacustrine deposits. A notable carbonate marker is the Long Point Bed, part of the Parachute Creek Member of the Green River Formation, which indicates a transition from freshwater to brackish water conditions during an early transgressive phase before the lake became saline. During this period, freshwater mollusks thrived, as evidenced by abundant fossils in the carbonate layer [17]. This information aids in understanding the organic material present during different phases of the lake's evolution. The evolving geology of ancient Lake Uinta was instrumental in forming oil reservoirs across the Uinta Basin. For example, the northern part of the lake was deeper than the southern part, resulting in higher depositional loads and more over-pressurized rocks [18].

2.1. The Duchesne Fault Zone

The Uinta Basin is deformed by a series of east-west striking dip-slip normal faults and parallel joints known as the Duchesne Fault Zone (DFZ), as shown in **Figures 2** and **5**. The origin of the DFZ is probably linked to the reactivation of pre-existing basement structures that occurred during the Laramide Orogeny in the Eocene [5,6]. However, this deformation contradicts the decrease downwards of displacement, which either terminates at 1,400 m depth or shallows into a north-dipping, low-angle detachment along bedding planes at 1,000 m [3]. The net displacement at the surface is 200 m [3]. The intense fracturing in the DFZ is believed to have enhanced oil production in the basin [5]. However, structural compartmentalisation within the central part of the fault zone could reduce long-term production rates with conventional vertical drilling. Tar sands along the DFZ likely provide evidence of upward fluid flow, while northwest- and west-trending gilsonite veins in the southeast of the Uinta Basin are due to hydraulic extension fracturing [1,19]. The gilsonite veins are thought to originate from hydrocarbons within the Mahogany Shale (**Figure 4**), indicating they are younger than Eocene. Cross-cutting relationships show they are older than the overlying Tertiary sediments, suggesting a likely Miocene emplacement [20]. Small, intact fragments of gilsonite within the DFZ reveal that the zone had become inactive before the injection of gilsonite into preexisting fractures.

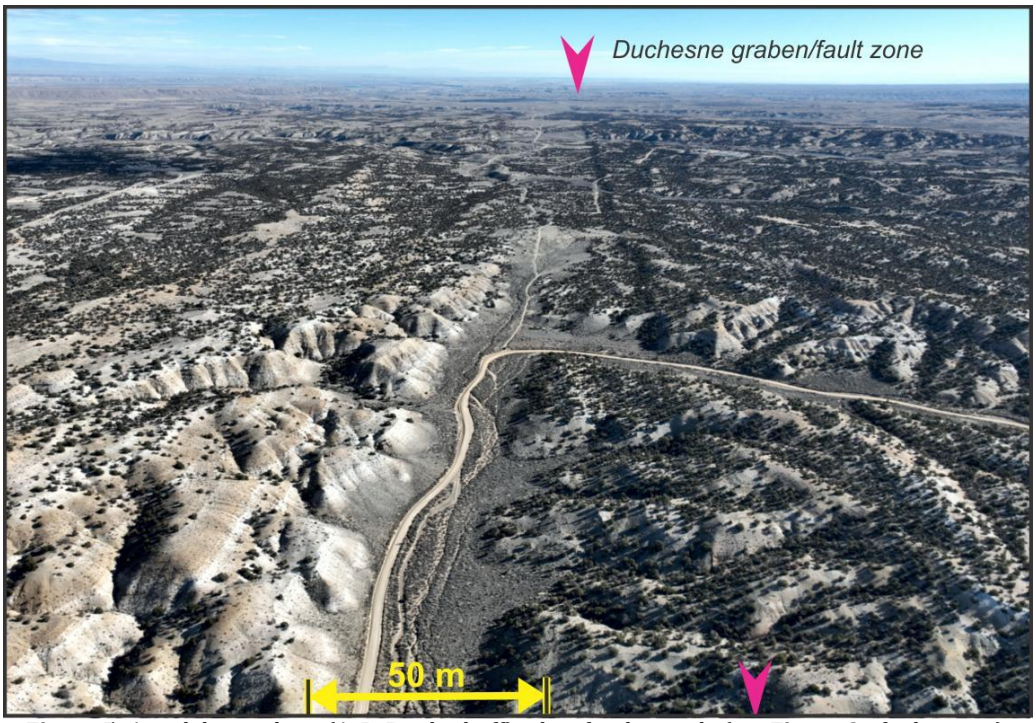

Figure 5. Aerial drone photo (A. R. Brinkerhoff) taken for this study (see **Figure 3a** for location).

Note: Altitude is 366 m above the ground surface of the Duchesne graben, facing east, located 4.8 km south of the town of Duchesne (**Figure 2a**).

2.2. Geochronology of the Duchesne Fault Zone

The deformation history of the DFZ, which cuts Eocene strata of the Green River, Uinta, and Duchesne River Formations (**Figure 4**), is polyphase, recording a complex evolution from Laramide-era contraction, including oblique reverse movement to Neogene extension. Evidence of Quaternary reactivation is debated. The timing of the structural evolution of the DFZ can be divided into three primary phases. The initiation of the DFZ is linked to the Laramide orogeny, likely reactivating a Palaeozoic or Proterozoic inherited structure. During the Eocene, the fault zone acted as a hinge line facilitating differential subsidence during the deposition of the Green River Formation [8,12]. The strike-slip component phase was synchronous with the broader uplift of the Uinta Mountains and basin subsidence. Following Laramide contraction, during the Oligocene–Miocene, the stress regime shifted to regional extension. The DFZ was reactivated as a normal fault system, creating the prominent graben topography visible today. Slickenside data from this interval indicate predominantly dip-slip movement, which overprints earlier strike-slip indicators [8,12]. The fault zone is classified as a "suspected" Quaternary fault (Class B) by the Utah Geological Survey. Scarps displacing Quaternary surfaces have been identified, which have been interpreted to be associated with Holocene activity (<10 ka) or late Pleistocene movement (<160 ka) [2,21]. However, conflicting interpretations exist; while some scarps align with fault traces, others may be erosional fault-line features resulting from differential erosion of the Eocene bedrock rather than tectonic surface rupture [2]. Definitive paleoseismic trenching data to confirm the timing of the most recent event are currently lacking.

The maximum age of the most recent significant offset along the DFZ is constrained by the youngest faulted bedrock units. High-precision $^{40}Ar/^{39}Ar$ dating of tuffaceous beds provides definitive age control for the middle Duchesne River Formation. Single-crystal laser fusion analyses yield ages of 39.47 ± 0.16 Ma (plagioclase) and 39.36 ± 0.15 Ma (sanidine) for tuffs located within the Dry Gulch Creek and Lapoint Members [22]. These dates, which are statistically indistinguishable, constrain the Duchesnean North American Land Mammal Age (NALMA) to approximately 39.4 Ma and confirm that the primary extensional displacement defining the

modern graben morphology postdates the late Eocene. The chemical and mineralogical "fingerprint" of the tuffs links them to the Northeast Nevada Volcanic Field, located roughly 400 km west of the Uinta Basin. The tuffs are rhyolitic fallout ash containing phenocrysts of quartz, biotite, sanidine, plagioclase, and allanite [22].

Detrital zircon fission-track thermochronology from the uppermost unit of the Duchesne River Formation, the Starr Flat Member, and the overlying Bishop Conglomerate further constrains the timing of basin fill and subsequent deformation. Zircon fission-track populations from the base and top of the Starr Flat Member yield ages ranging from 36.7 ± 3.9 Ma to 30.0 ± 1.5 Ma [23]. These cooling ages, derived from the exhuming Uinta Mountains source terrane to the north, suggest that deposition of the Starr Flat Member—and therefore the subsequent faulting that offsets it—continued into the early Oligocene (approx. 30 Ma).

Additionally, $^{40}Ar/^{39}Ar$ ages of sanidine from the base of the Bishop Conglomerate range from 34.03 ± 0.04 Ma to 30.54 ± 0.22 Ma [24]. The stratigraphic relationship between the DFZ and the Bishop Conglomerate remains a key structural marker; where the fault zone cuts these Oligocene units, it confirms that extension continued into or post-dated the Oligocene.

2.3. Regional Tectonic Context for the Duchesne Fault Zone

The initiation of the DFZ is contemporaneous with the late stages of the Laramide orogeny, a period of basement-cored uplifts and peripheral basin subsidence that defined the Rocky Mountain foreland from approximately 70 to 34 Ma [25,26]. During the Eocene, the DFZ functioned as a structural hinge line separating the rapidly subsiding northern Uinta Basin—adjacent to the rising Uinta Mountains—from the shallower, more stable southern basin limb [3]. Subsurface analysis of the Green River Formation indicates that the fault zone accommodated differential subsidence and syndepositional deformation, characterised by oblique slip and localised uplift [8]. This contractional phase is recorded in the folding and faulting of Eocene strata, including the Green River and Uinta Formations, which show evidence of strike-slip and oblique-slip kinematics consistent with the regional Laramide stress field [9].

The syn-orogenic sedimentary record provides key constraints on the unroofing and cooling history of the Uinta Mountains Laramide uplift. The Duchesne River Formation, which is cut by the DFZ, contains a distinct "unroofing sequence" marked by an upward stratigraphic increase in Proterozoic quartzite clasts and a decrease in Palaeozoic carbonate clasts, recording the progressive erosion of the core of the Uinta Mountains [27]. Thermochronologic data, specifically zircon fission-track ages from the overlying Bishop Conglomerate and upper Duchesne River Formation, yield cooling ages between ca. 36 and 30 Ma [24,28]. These ages, along with high-precision $^{40}Ar/^{39}Ar$ dates of ~39.4 Ma from tuffs within the faulted Duchesne River Formation [22], indicate that significant exhumation and relief generation continued into the late Eocene and early Oligocene, overlapping with the cessation of Laramide compression.

Following the Laramide orogeny, the regional stress regime shifted to east-west extension, a tectonic transition that also drove the development of the Wasatch fault zone to the west [29]. The DFZ was reactivated as a system of *en echelon* normal faults and grabens during this extensional phase, likely in the Oligocene and Miocene [1]. While the Wasatch fault zone represents the primary structural boundary between the Basin and Range and the Middle Rocky Mountains, the DFZ records intra-basin extension that accommodates strain within the Colorado Plateau–Basin and Range transition zone. The graben morphology visible today, which offsets the Eocene bedrock, is primarily a result of this Neogene extension, with some studies suggesting potential reactivation into the Quaternary [2,29].

2.4. Biostratigraphic Constraints on Deformation Timing of the Duchesne Fault Zone

The timing of deformation in Laramide Orogeny settings is frequently constrained by the biostratigraphic analysis of syn-orogenic sedimentary units, particularly where lacustrine and fluvial facies interfinger. In the Uinta Basin, the DFZ cuts a thick sequence of Eocene strata, in which the transition between the lacustrine Green River Formation and the overlying/interfingering

fluvial Uinta and Duchesne River Formations records the complex interplay between basin subsidence and structural reactivation. High-resolution biostratigraphy within these "sandstone-limestone facies" (**Figure 4**) provides critical maximum-age constraints on the onset of brittle deformation and helps resolve the chronology of the Laramide-compression-to-extension transition.

The Lower Green River Formation (Eocene, ~52–49 Ma), often mapped as the "sandstone and limestone facies" in the vicinity of the DFZ, contains abundant, well-preserved biostratigraphic markers that pinpoint the age of the host rock displaced by subsequent faulting. For instance, avian fossils such as *Gallinuloides wyomingensis*, provide a distinct Early Eocene biostratigraphic datum (~52 Ma) within the lacustrine limestone beds [30]. Similarly, the recent discovery of early insects, specifically *Eornithoica grimaldii*, in the Lower Green River Formation offers high-resolution temporal control, dating these specific horizons to approximately 52 Ma [31]. These fossils establish a robust maximum age for the cross-cutting extensional faults of the DFZ, confirming that the primary graben-forming deformation occurred post-Early Eocene.

In the Duchesne 30′ × 60′ quadrangle, the "sandstone and limestone facies" is directly cut by the east-west trending normal faults of the DFZ [1]. The biostratigraphic ages derived from the rich fossil assemblages in the limestone interbeds constrain the timing of the underlying crustal stability prior to the faulting event. Furthermore, mammalian biostratigraphy in the overlying sandstone-dominated Uinta and Duchesne River Formations—characterised by the Uintan and Duchesnean North American Land Mammal Ages (NALMAs)—brackets the cessation of Laramide compressional folding and the onset of the extensional regime that generated the modern DFZ topography [32,33].

2.5. Oil and Gas Production

When ancient Lake Uinta entered its closed-lake stage, carbonate and secondary silica precipitated, forming fine-grained, organic-rich source rocks that cover the Uinta Basin. During the Eocene, Lake Uinta was chemically stratified, resulting in multiple distinct nutrient layers within the water that created a favourable environment for organic material preservation. This led to the formation of bituminous shales, which served as source rocks for hydrocarbon veins that later cut through the surrounding rock. Sandstones in contact with the oil shales absorbed oil seepage and became saturated reservoirs [34].

The Uinta Basin is Utah's largest hydrocarbon-producing region, primarily due to multiple source rocks with fracture permeability. Fracturing increases within a breached anticline of the DG, a structural half-graben in the western part of the DFZ [3] (**Figures 1, 3,** and **5**). Data from wells within the fault zone show higher oil production near the northern end of the DFZ compared to the less productive southern end. Oil grades range from viscous, asphalt-rich black oil to bright yellow oil with a high gas-to-oil ratio (GOR). Higher thermal gradients correlate with increased GOR and decreased asphalt content. No asphalt-rich oil has been commercially viable [14]. The over-pressured sections of the DFZ are mainly located within the Coltan Formation and the Flagstaff Member of the Green River Formation [35] (**Figure 4**).

2.6. Neutral Surface Partitioning Strain along the Duchesne Fault Zone

We propose that the DFZ developed synchronously with the Laramide-age Duchesne Anticline, originating from strain partitioning across a neutral surface within the fold structure, consistent with a bending-beam model (**Table 2**). The coexistence of extension and contraction within a single folded layer is primarily governed by the mechanism of Tangential Longitudinal Strain (TLS). This mechanism, often associated with the buckling of competent layers (parallel or Class 1B folds), requires redistributing strain to accommodate curvature while maintaining layer thickness [36,37]. In an ideal TLS model, deformation is accommodated by pure shear, where the strain axes are oriented tangentially and normal to the layer boundaries. As a competent layer buckles, the strain distribution effectively decouples across a surface of zero finite longitudinal strain, known as the neutral surface [38]. The material layers located on the convex side of the neutral surface undergo tangential elongation (extension) parallel to the layering. Conversely, material on the concave side of the neutral

surface is subjected to tangential shortening (contraction) [39]. This strain geometry implies that a rock unit folding under regional contraction can paradoxically exhibit extensional features if the observation is limited to the upper hinge zone [40]. Further, this vertical partitioning of strain is scale-independent [41].

Table 2. Features of Three Depth Zones in a Bending Beam Model for the Duchesne Fault Zone.

Section	Structural Features	Dominant Stress State (Depth)	Strata Involved	Lithology	Character
Upper Zone	Normal faults, *en echelon* grabens	Extension (0 to 1,000 m)	Uinta Fm, Upper Green River Fm (Sandstone-Limestone Mbr)	Massive sandstones, siltstones	Brittle failure: wide, open fractures (often filled with gilsonite) and high-angle normal faults
Neutral Surface	Fault displacement dies out downward	Zero strain (very thin, transition at ~930–1,365 m)	Green River Fm (Parachute Creek Mbr)	Oil shales, marls	Transition zone where faults die out with depth. This is the pivot point of the bending beam
Lower Zone	Folding, tight drape folds	Compressional (>1,500 m)	Lower Green River Fm (Saline facies)	Oolitic limestones, fluvial sandstones.	Broad, gentle anticlinal folding; tight fractures; no significant vertical fault offset

Sources: Groeger and Bruhn [3], Brinkerhoff and Sprinkel [4], Utah Geological Survey [6], and Smith [10].

2.7. The Duchesne Graben

An essential feature of the basin is the Duchesne Graben (DG), an extensional half-graben located above the neutral surface of the Duchesne anticline [4] (**Figure 1**). Faulting in the southern part of the DG is more extensive than in the northern part, with the hanging wall being closer to the basin-bounding fault. Bedding within the graben dips at angles of 4–6° and 8–11° toward the NNE [4]. Normal faulting along the graben's edges produces N–S dipping bedding in the horsts within the trough (**Figure 6**). Strata within the fault zone predominantly feature joints that strike E–W, parallel to the normal faults, and are filled with calcite veins [4].

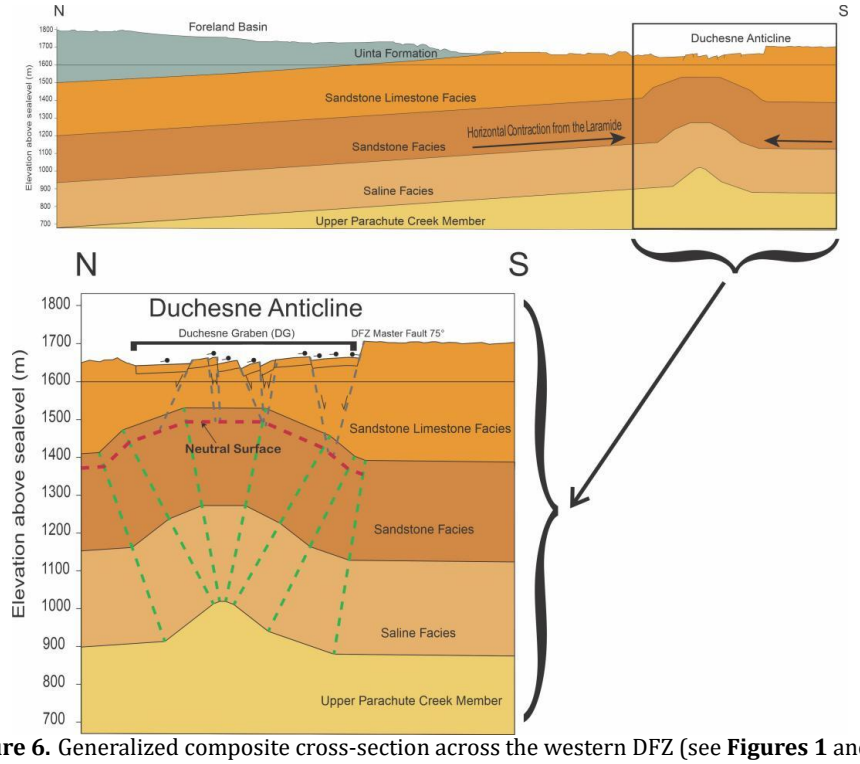

Figure 6. Generalized composite cross-section across the western DFZ (see **Figures 1** and **2**).

Note: The enlarged bottom area emphasizes the relationship between the Duchesne Anticline, the reverse fault- cored folding within the saline facies, and the DG. The blue bracket marks the location of the DG fault, where north- and south-dipping horst blocks show minimal slip and may serve as seals against fluid movement. Attitude symbols above the strike and dip measurement areas indicate dip direction. Green dashed lines represent dip domains of the Duchesne Anticline, while dashed grey lines illustrate normal faulting from the DG.

2.8. Comparison of Deformation Models

Groeger and Bruhn[3] observed that displacement on the Duchesne Graben was absent in well logs below 1,365 m, and possibly also above that depth. They proposed two models to explain this: a planar model, in which fault displacements decrease with depth and eventually cease (**Figure 7a**), and a detachment model, in which displacement on graben bounding faults is transferred onto a detachment, likely along a bedding plane (**Figure 7b**). The work of Groeger and Bruhn[3] was based on subsurface data and outcrop measurements in the centre of the Duchesne fault zone. Further work has shown that several fault zones in the Uinta Basin exhibit displacements that quickly diminish with depth, such as the Sand Wash and Devil's Canyon fault zones (Subsection 5.3). Fieldwork associated with this project also noted that the base of the Duchesne Graben is exposed on the eastern wall of Lake Canyon (**Figure 2**), and much deeper within the canyon, folding and minor reverse faults are present, directly underlying the graben (**Figure 8**). The Lake Canyon outcrops directly support Groeger and Bruhn's[3] original planar model.

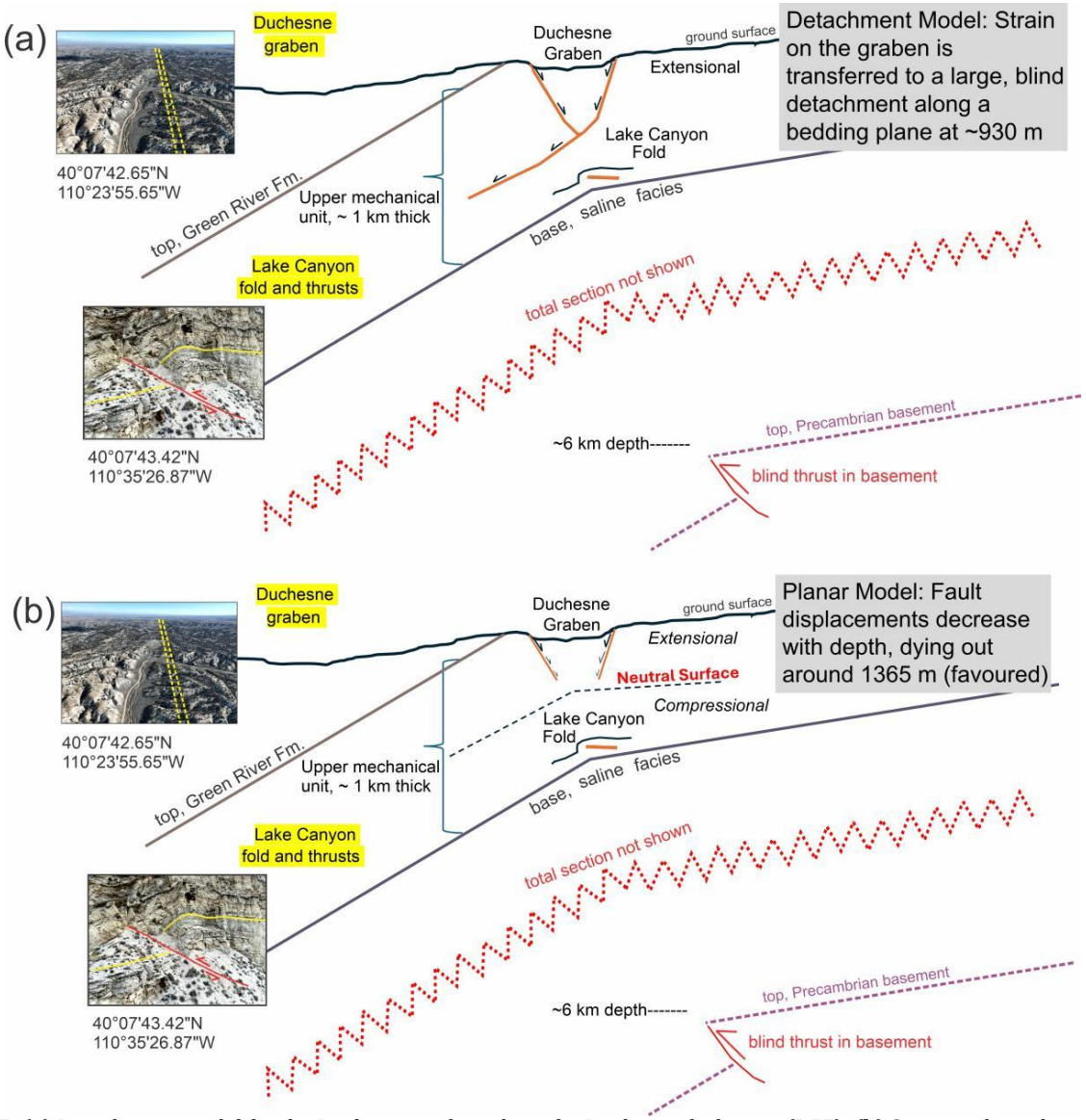

Figure 7. (**a**) Detachment model for the Duchesne graben along the Duchesne fault zone (DFZ); (**b**) Same as above, but showing planar faulting in a bending beam model with a neutral surface.

Note: The respective grabens in each fault zone are interpreted as shallow extensional features draped above a larger, deeply buried reverse fault and sedimentary section. In both cases, the weak, organic-rich, lacustrine shales easily accommodated slip, allowing the extensional strain to be concentrated in the narrow grabens as observed at the Earth's surface.

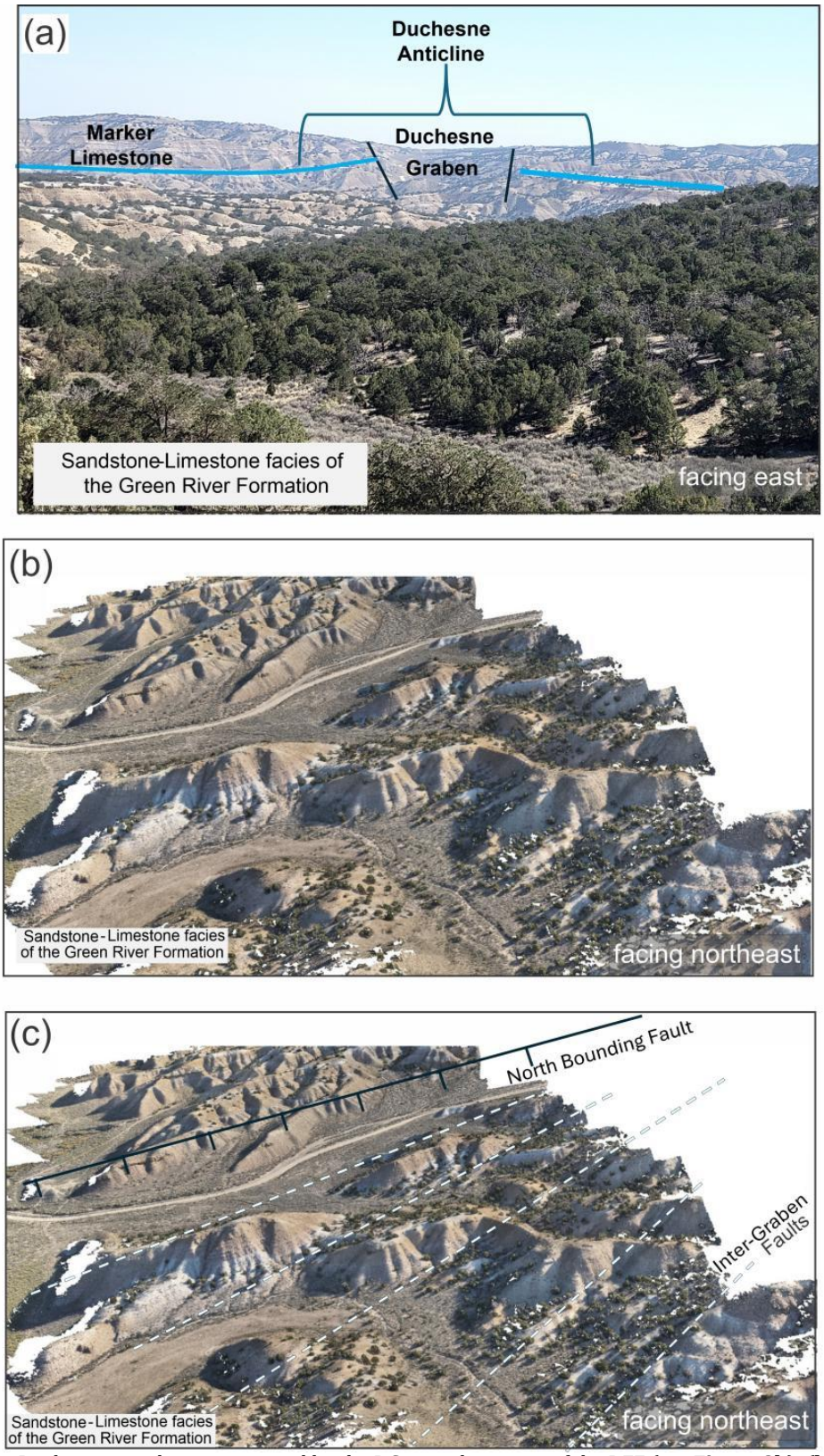

Figure 8. (**a**) The Duchesne anticline is separated by the DG near the center of the DFZ (see **Figure 2b**); (**b**,**c**) The interpreted and uninterpreted photogrammetry models of the DG located within the crest of the Duchesne Anticline depicted in the previous image.

Note: The blue marker bed in **Figure 8a** indicates a low-angle dip along the north-bounding fault of the DG. The blocks within the DG show heavy faulting and fracturing. Refer to **Figure 2b** for location.

3. Methodology

To gain a better understanding of the geometry of the underlying geology and its impact on petroleum production, multiple methods were employed to reconstruct the geological history. These include geometric analyses using stereographic projections of bedding and fault planes, cross-sections, photogrammetry models, a dedicated LiDAR survey, and construction of subsurface structural and isochore maps from regional drillhole data. The combination of these methods helps to uncover the structural history of the lower Green River Formation (**Figure 4a**) within the DFZ. This formation is especially significant because it is one of the largest oil-producing reservoirs in Utah [7,9].

3.1. Photogrammetry and LiDAR

A DJI Phantom 4™ drone, equipped with a 20-mm, 4-megapixel camera, was employed to investigate stratigraphic exposures on the surface within the Duchesne anticline and the DG in the DFZ (**Figures 3, 5,** and **6**). Agisoft Metashape™ software processed the drone imagery into medium-resolution mesh and texture models, which were then exported as a PNG file. For the LiDAR survey (**Figure 3b**), we used a DJI Matrice 350 RTK drone, with a DJI Zenmuse L2 LiDAR camera. The LiDAR data set consists of 12,780 and 7,739 grid points in the X and Y directions (98,904,420 points, total), respectively, with a point separation of 0.368351678 m. The survey fits into a rectangle (**Figure 3b**) with an area of approximately 2,918,265 m^2.

3.2. Measuring Strike and Dip

Measurements of strike and dip were collected using FieldMove Clino™. These measurements encompassed bedding planes, faults, slickenlines, and joints. The data were combined to create stereographs that depict the geometric relationships of bedding and fault planes in folds and extensional faults within the DFZ. All measurements originate from the member B facies, sandstone limestone facies, and saline facies (**Figure 4a**). Stereographs were generated by exporting strike and dip data from FieldMove Clino™ as CSV files, which were then processed using Python™ in Google Colab™.

3.3. Construction of a Geological Cross Section

A cross-section was produced in Adobe Illustrator 2024™. Bedding dips within the DFZ and Duchesne anticline were gathered from FieldMove Clino™ measurements collected in the field. Dip directions north and south of the DFZ within the associated flexural basin were obtained from Utah Geological Survey [6]. Formation widths were sourced from Sprinkel [1]. Dip angles of the DG were extracted from Groeger and Bruhn [3].

4. Results

The DFZ comprises several structural features vital to petroleum reservoir development. These include the shallow-dipping Duchesne anticline from the Laramide era, deformation bands [41] within horizontally compressed folds, and grabens that enable faulting and fracturing. The composite cross-section (**Figure 6**) indicates that the varying stress regimes within the Duchesne anticline and the larger DFZ originated from a single orogenic event.

4.1. LiDAR Imagery

A LiDAR survey was acquired over the western part of DFZ and DG (**Figure 5**), to investigate how these exceptionally straight features (**Figure 2d**) are expressed in high-resolution topography (**Figure 3a**), especially considering how they are seen on satellite imagery as colour changes in surface soils and rocks (**Figure 3a**). The LiDAR image (**Figure 3b**) alone does not show an obvious lineament. The elevation slope map (**Figure 3c**) shows an alignment of alternating high and low values (dark and light colours, respectively, **Figure 3c**) along the trace of the DFZ. This behaviour is supported by elevation curvature (**Figure 3d**), which shows an alignment of anomalous values. A vector representation of curvature (**Figure 3e**) accentuates the expression of the DFZ as a discontinuity. Elevation profiles extracted from the LiDAR survey (**Figure 3f,g**) clearly indicate a topographic inflexion corresponding to the DFZ trace, with a

high degree of variation.

4.2. Duchesne Anticline

A total of 152 strike and dip measurements of bedding and fault planes were documented within the DFZ (see Ketring [42] for detailed data). The bedding planes of the Duchesne anticline dip both north and south, with dip angles ranging from 2° to 37°. The northern limb dips more steeply than the shallower southern limb, indicating an asymmetrical fold (see **Figure 8**). Most measurements were taken in the sandstone-limestone and saline facies (see **Figure 4a**). Bedding measurements above the northernmost accommodating fault of the DG in Indian Canyon, along with bedding planes in the saline facies within Lake Canyon, suggest that the Duchesne anticline has low dip angles (see **Figure 6**). The 37° dips are only on rotated fault blocks within the Duchesne Graben. The fold that hosts the graben is much broader, but its back limb and forelimb have dips of 2° and 6°, giving a rough curvature of 4°. Using our measured values, the portion of the Green River Formation above the fold's neutral surface and experiencing extension is about 1.5 km thick, and the fold itself is about 2 km. This broad fold has a large calculated radius of 28 km, and the outer margin would have undergone 5.2% extension. The resulting fault that would accommodate this extensional strain, if concentrated on a single fault, would have around 180 m of throw, assuming the entire length of the fault maintains the 60° dips we measure at the surface. **Table 3** compares the changes in stratigraphic throw for the central and eastern DFZ. The crest of the Duchesne anticline spans almost the entire DFZ, starting near the western boundary of the fault zone and gradually narrowing as it extends eastward along the anticline's trend (see **Figure 8**). Additionally, tar sand exposures are found along the eastern section of the DFZ.

4.3. Reverse Faulting

Within the saline facies of the Green River Formation, reverse faults related to anticlinal folding are found along the edges of the folds (**Figures 9** and **10**). These faults tend to be low-angle and show minor displacement near the saline facies folds. The low-angle reverse faults stem from the Laramide Orogeny, with displacement generally limited to a few centimetres [3].

As elevation increases, the horizontal contraction causes the dip of the bedding plane in the saline facies to increase. This change stems from the primary accommodating fault located near the top of the saline facies. The fault zone is heavily fractured and segmented because of fault drag (**Figure 11**). Signs of fault drag are evident next to the main accommodating fault, where horizontal faulting occurs alongside vertically oriented bedding. On the larger scale fold, the reverse faults are either parasitic on the limbs, or core the folds with rather small offsets (10 m or less).

Table 3. Stratigraphic Throw across Central DFZ (Indian Cyn) & Eastern DFZ (Lake Cyn).

Throw	Central DFZ	Eastern DFZ
Fault morphology	Continuous, well-defined master faults	En echelon, segmented faults
Neutral surface depth	Deepest (~1,200 m–1,400 m)	Shallower (~900–1,100 m)
Dominant strata	Uinta Fm & Parachute Creek Mbr	Upper Green River Fm (Transition facies)

Sources: Sprinkel [1], Groeger and Bruhn [3], Brinkerhoff and Sprinkel [4], and Utah Geological Survey [6].

4.4. Normal Faulting

Normal faults along the Duchesne anticline's margin dip both north and south. In the DFZ, the average true dip of these faults is 51° N. Slickenlines show dip-slip movement. In the DG, block-bounding faults also dip in both directions (north and south; **Figure 12**) at angles from 2° to 37°. The variety of dip directions in the DG, along with the wide range of normal fault dips and slickenline orientations, indicates block rotations within the DG (**Figure 13**).

4.5. Block Faulting along the Margins of the Duchesne Graben

Within the central DG, horsts are defined by N-S-dipping faults. Strike and dip data for these normal faults were compiled from Morgan et al. [16]. The faults display true dips ranging from 53.6° N to 77.7° N. A sin-

gle horst block can show multiple bedding dip directions (see **Figure 14**). This variation results from segmentation caused by normal faulting during extension above the neutral surface (refer to **Figure 6**). Evidence of this tectonic activity, which leads to segmentation, is present at the southern edge of the DG, where surface exposures of the escarpments show a north-dipping fault and south-dipping beds (see **Figure 15**).

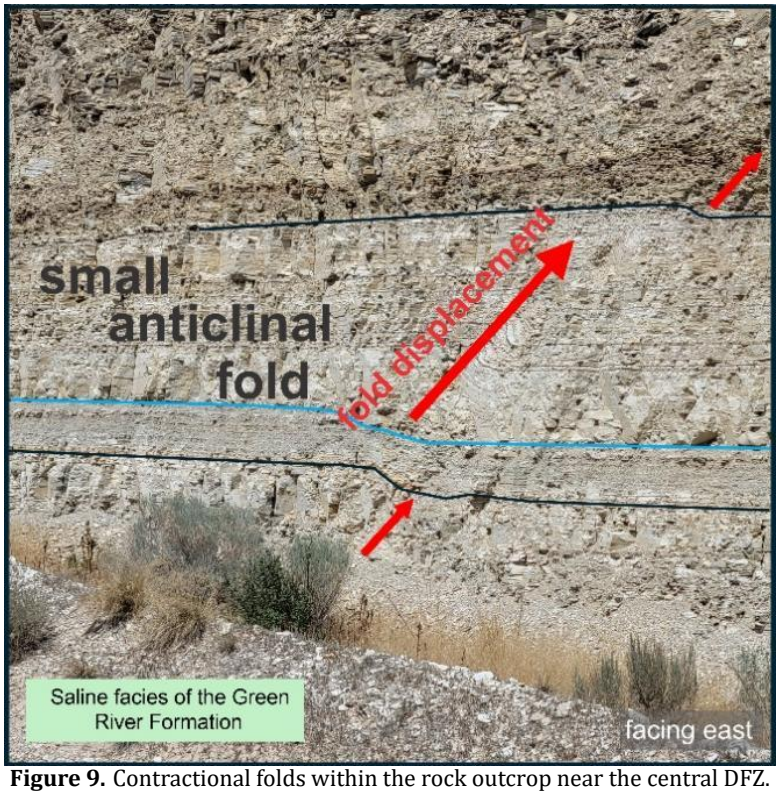

Figure 9. Contractional folds within the rock outcrop near the central DFZ.

Note: The fold shows minor displacement, evinced by deformation bands. See **Figure 2b** for the location.

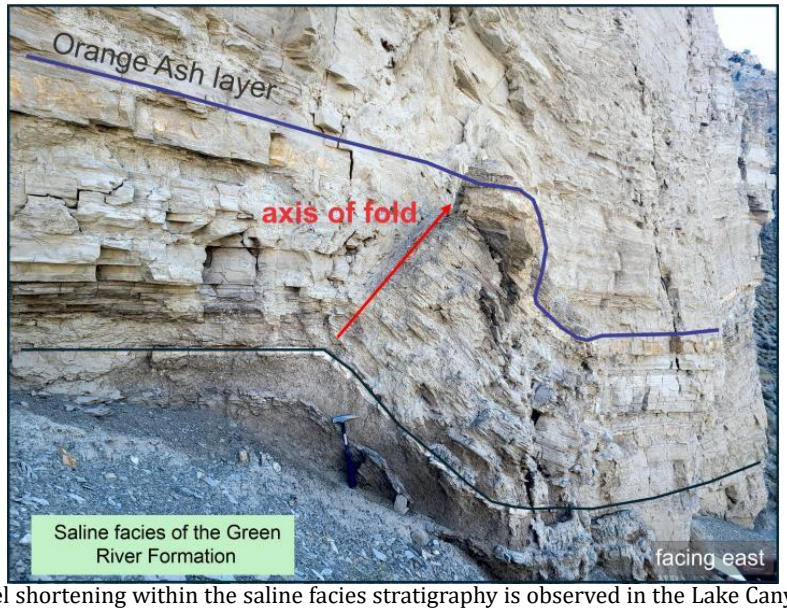

Figure 10. Layer parallel shortening within the saline facies stratigraphy is observed in the Lake Canyon folds. See **Figure 2b** for the location.

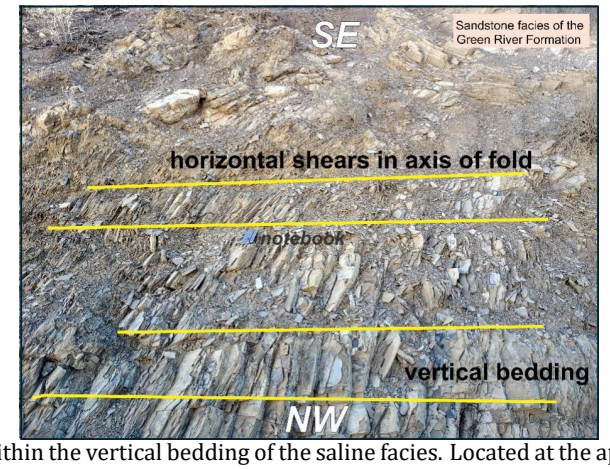

Figure 11. Horizontal faulting within the vertical bedding of the saline facies. Located at the apex of the fold beneath the neutral surface. See **Figure 2b** for the location.

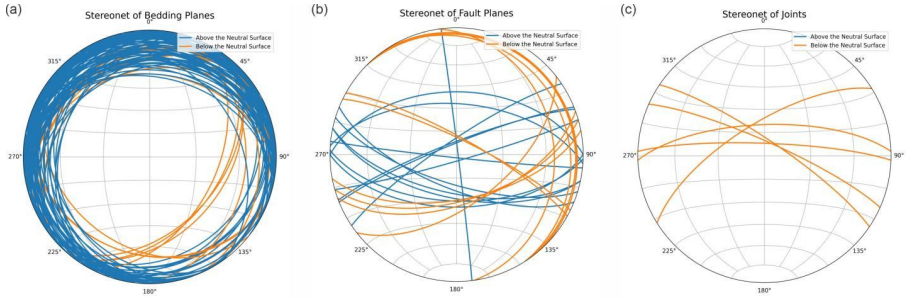

Figure 12. Stereographs for the DFZ. Individual units are distinguished by colour. (**a**) The bedding plane dips, as recorded from surface exposures within the Duchesne Anticline, show shallow-dipping beds that range from 2° to 37°; (**b**) The steeper faults observed in the sandstone limestone facies and member B facies above the neutral surface are normal faults, whereas the shallow faults within the saline facies below the neutral surface are reverse faults; (**c**) Steep joint sets within the saline facies observed from deformation bands.

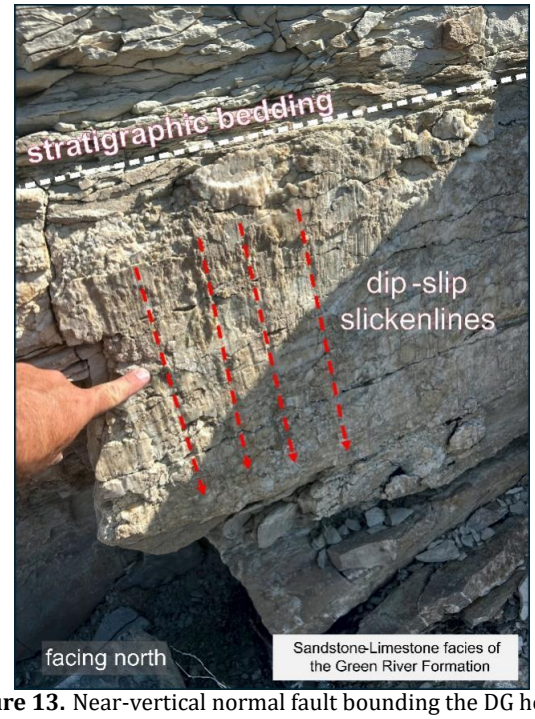

Figure 13. Near-vertical normal fault bounding the DG horsts.

Note: Red arrows indicate the direction of slip of slickensides within the stratigraphy. Slickensides plunge at 83°. See **Figure 2b** for the location.

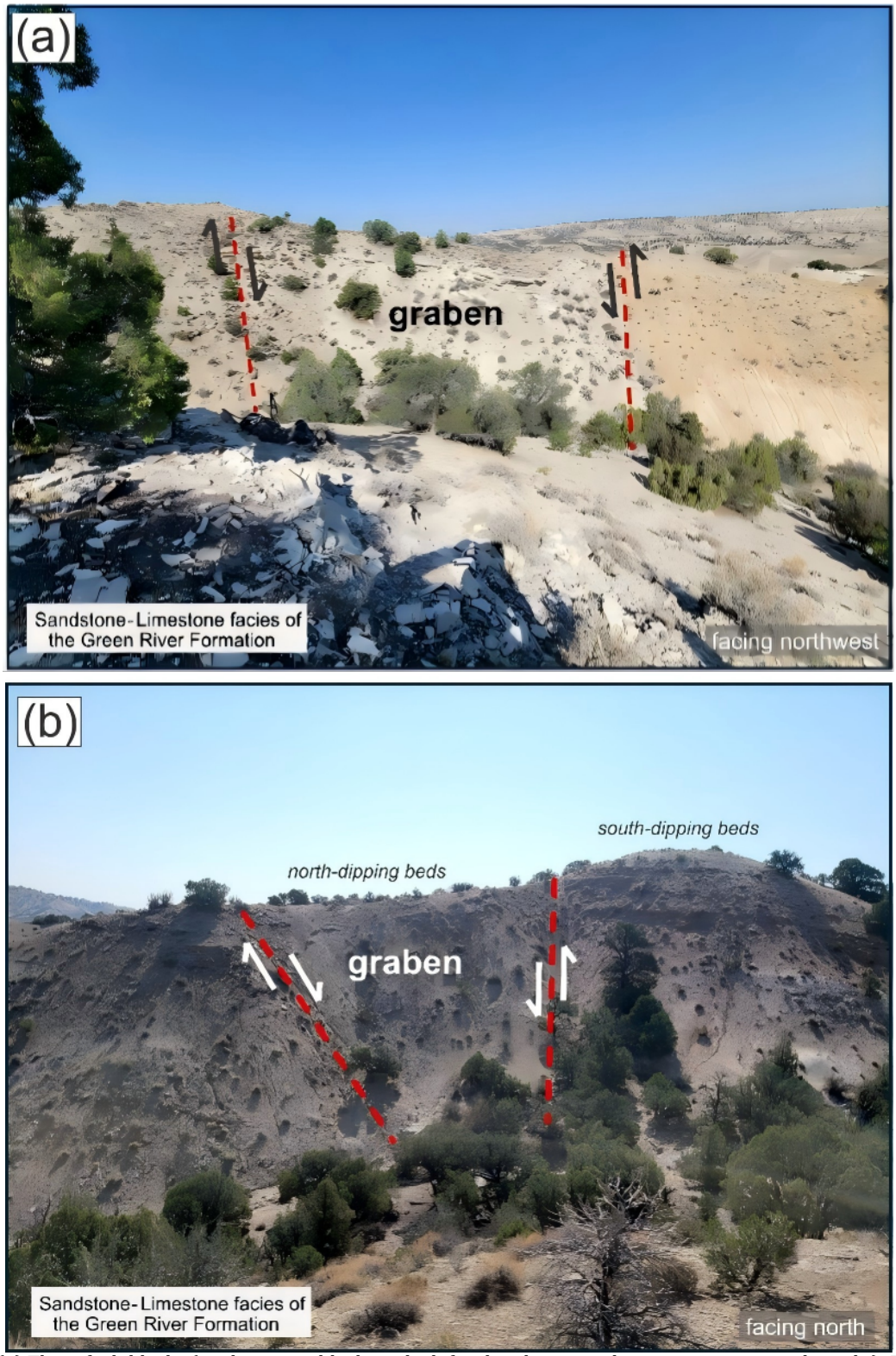

Figure 14. (**a**) Three fault blocks (medium grey block on the left, whitish grey in the centre, orange on the right). The block on the left dips south, while the block on the right dips north. In the centre, one block collapsed downward, with the others spread apart. There is a drag on the dip on the right side of the centre block; (**b**) Faulted horst blocks on the southern bounding fault of the graben. On the right, a south-dipping block; in the centre, a north-dipping block. See **Figure 2b** for the location.

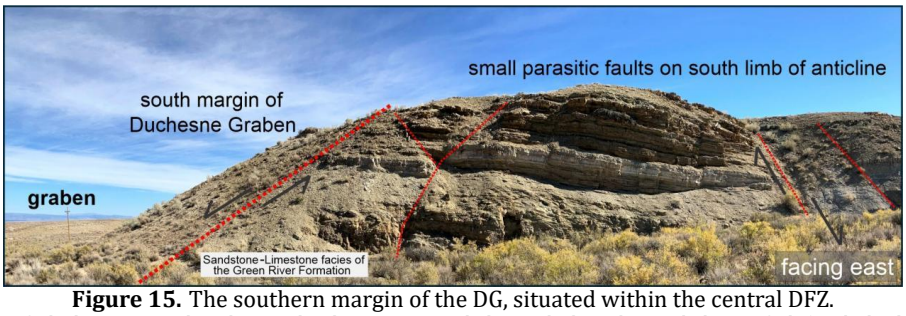

Figure 15. The southern margin of the DG, situated within the central DFZ.

Note: It is interpreted as a faulted escarpment, heavily jointed and containing south-dipping beds, with a north-dipping fault (marked in blue). The opposing dips along the southern margin of the DG highlight the structures responsible for the N-S dipping horsts in the central DG. See **Figure 2b** for the location.

4.6. Subsurface Mapping

Stratigraphic tops within the Green River Formation (**Figure 4a**) were picked within subsurface mapping software (GeoGraphix 2024.1™) (**Figure 16**). These tops were then used to correlate surfaces across the central Uinta Basin (**Figure 16a**) with a focus on the Duchesne fault zone, resulting in a sub-sea structural contour map (**Figure 17b**). Note the surface traces of the Duchesne fault zone are drawn as red lines running roughly east-west, and that the tightest contours, related to the steepest structural dips, are associated with the fault zone. To better illustrate the increase in stratigraphic dip and structural folding near the Duchesne fault zone we calculated a first derivative of the structural surface map from **Figure 17b**. The first derivative of a structure map calculates the stratigraphic dip angle of that surface (**Figure 17d**). Note that the steepest calculated dips are associated with the Duchesne fault zone, especially its west side, where the grabens are widest and best developed. Steeper folding on the west side of the structure is associated with greater extension of the overlying sediments, expressed as the Duchesne graben. We also calculated several isopach maps of Green River stratigraphy (**Figure 4a**) that was deposited contemporaneously with movement on the Duchesne fault zone. An isochore of the Douglas Creek Member of the Green River Formation (**Figure 17d**) shows significant thickening on the downward-thrown (basinward) side of the fault zone. We interpret the stratigraphic thickening into the basin as sediments encountering greater accommodation related to movement on the fault zone. The DFZ acted as a hinge point in the developing Uinta Basin, with steeper stratigraphic dips to the north of the fault zone (**Figure 16**). Today, the DFZ marks the southern boundary of the deep, overpressured part of the Uinta Basin petroleum system.

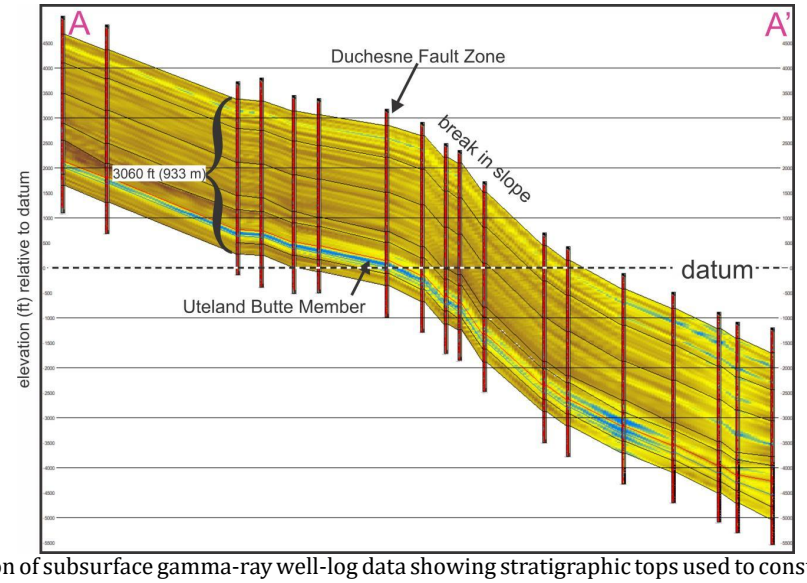

Figure 16. Cross-section of subsurface gamma-ray well-log data showing stratigraphic tops used to construct the maps in **Figure 17**.

Note: The cross-section demonstrates the DFZ's influence on the greater structural and depositional trends in the Uinta Basin.

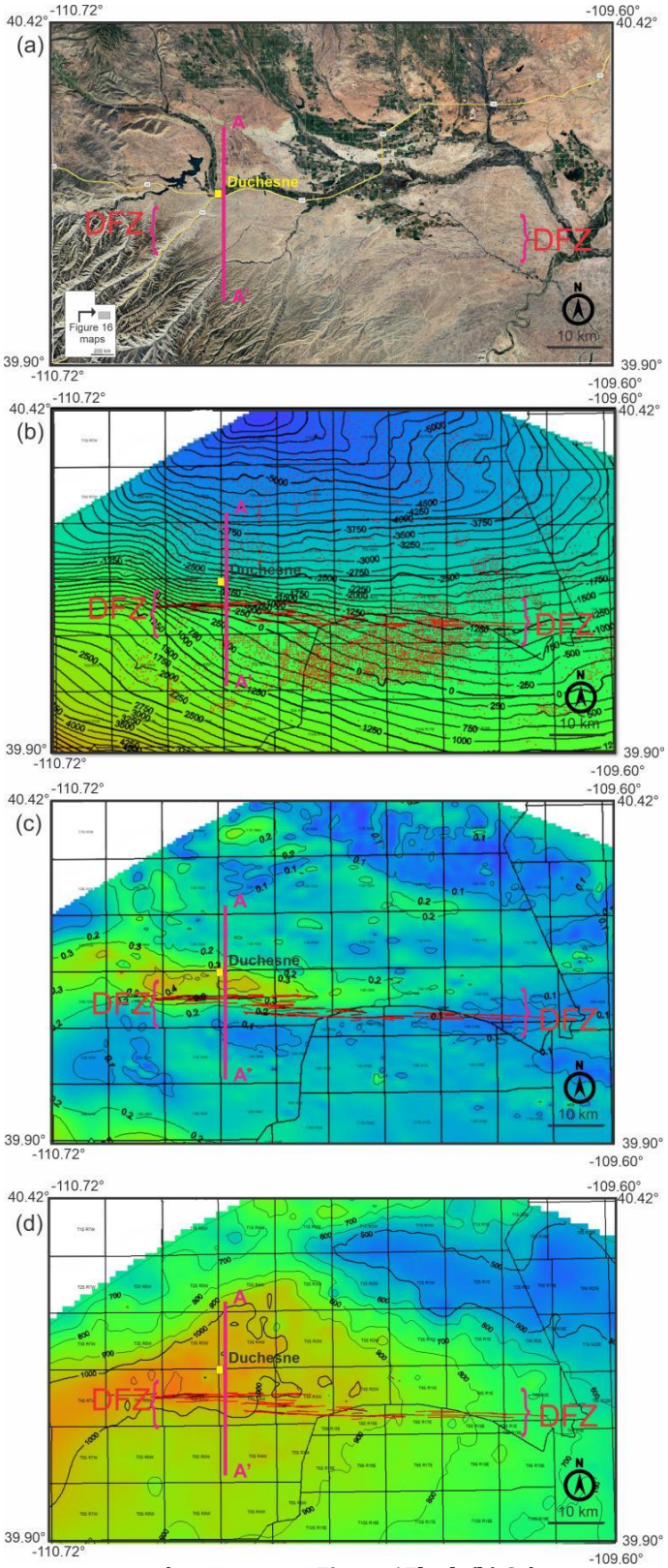

Figure 17. (**a**) Google Earth image corresponding to areas in **Figure 17b**–**d**; (**b**) Subsea-true-vertical-depth (SSTVD) structure contour map on the top of the Uteland Butte member of the Eocene Green River Formation (**Figure 4a**); (**c**) First Derivative (dip-direction calculation) of the structure map surface from **Figure 17b**; (**d**) Isopach thickness of the Douglas Creek Member of the Green River Formation (**Figure 4a**).

Note: A–A' marks the location of the well-log cross-section in **Figure 16**. DFZ is Duchesne Fault zone; The contour interval in **Figure 17b** is 250 ft (76.2 m); The contour interval in **Figure 17c** is the stratigraphic dip angle; The contour interval in **Figure 17d** is 100 ft (30.5 m).

5. Discussion

5.1. Structural Influence on Petroleum Production

For the compartmentalisation hypothesis to be credible, the DFZ must contain structures that restrict fluid flow. These include blind reverse faults in basement crystalline rocks with overlying sediments, including the Green River Formation, deformed into a fold over the reverse fault; extension over the fold's neutral surface resulting in the Duchesne Graben, and superimposed extensional faults. Faulted regions exhibit permeability variations due to differences in porosity and rock strength. In the overlying sandstone, higher porosity and brittleness lead to fracturing, increasing permeability, as evidenced by the surface tar sands along fault strands. With deeper burial and higher temperatures, primary porosity decreases due to compaction and silica cement precipitating from fluids flowing through the faulted sandstones. Below the neutral surface, more ductile limestones develop low-displacement deformation bands that initially form conduits to vertical fluid flow, then become barriers to horizontal fluid movement when they become completely cemented. When faulting juxtaposes rocks with different properties, permeability typically decreases due to variations in mechanical strength and total porosity, which hinder fluid flow.

This study's aerial photography and surface strike-slip measurements indicate that the DFZ extends east-west and experiences north-south dip-slip extension (**Figures 8** and **12**). During Laramide shortening, the Duchesne anticline encountered varying stress conditions and fault activity, accommodating shortening through folding and localized faulting within the axial fold. The crest of the anticline was naturally susceptible to normal faulting due to extensional stresses above the neutral surface, where differential stress promoted the formation of small normal faults and fractures (**Figure 6**). These extensional features could have influenced fluid flow pathways by increasing fracture density in the rock layers, thereby enhancing permeability in the anticlinal structures.

The formation of Ancient Lake Uinta and the ongoing subsidence of the Uinta Basin created favourable conditions for the accumulation of oil-rich sediments. Laramide compression shaped anticlinal folds that acted as effective traps for petroleum. During the formation of the Duchesne anticline, extensional forces responsible for normal faulting at the crest also generated the DG, offering a pathway for fluid flow and hydrocarbon migration through related faults. The increased permeability in the bedrock facilitates fluid migration and extraction; however, south-dipping beds and north-dipping faults filled with clay-rich gouge and act as seals, limiting overall permeability. This sealing effect is strengthened by the low slip within the DFZ (**Figure 6**), which diminishes the development of high-permeability pathways. Since fault slippage typically enhances permeability, its restriction in the DFZ further impairs fluid flow.

The synchronous growth of the extensional DFZ and the Duchesne Anticline generated initial fractures that facilitated fluid migration, which were continually altered as folding progressed. In the eastern DFZ, evidence of fluid flow is apparent on the surface, such as oil staining in sandstones, silica cementation, and clay alterations. These pathways initially allowed fluid movement but eventually became barriers due to ongoing folding and fracture cementation. This transition is reflected in the production map from Brinkerhoff and Sprinkel [7], where small reservoirs caused wells to quickly reach bubble point, resulting in high initial production that soon declined. Additional cementation occurred through post-deformation processes like mineral crystallisation, evinced by silica cementation on the DFZ surface. Fault movement related to the Duchesne fault zone occurred relatively soon after burial and initial lithification, likely before the Oligocene epoch, as demonstrated by the cross-cutting relationship of Gilsonite dikes that extend across and into the Duchesne fault zone. Maximum petroleum generation took place in the early Miocene [10,13], significantly after the fault zone moved, allowing ample time for cementation to occlude faults, damage zones, and deformation bands.

We do not interpret the DFZ as a growth fault (defined as a shallow, listric fault that accumulates sediment as a footwall block slides basinward, rotating as it moves), but rather as a reactivated fault system that appears to have had intermittent movement in the

basement, Palaeozoic, and Mesozoic sections. Although the Green River Formation can experience stratigraphic thickening basinward of the DFZ, this is due to both the thickness of the Green River Formation (~1.5 km at the DFZ) and the varied nature of strain on the fault zone. Deeper members of the Green River Formation do indeed thicken basinward of the DFZ, as shown by subsurface well data, but the sediments affected by the Duchesne anticline are situated much higher in the stratigraphic section of the Green River Formation, impacting only a relatively small portion of it.

Limited fault slippage, indicated by deformation bands below the neutral surface and overlying extensional faulting influenced by fluid alterations, reduces reservoir connectivity. This complicates vertical drilling, as seen in the historical wells within the central DFZ [7]. A well that initially produces high output may become unproductive once these small, isolated (compartmentalised) reservoirs are depleted, causing pressure drops and early oil bubble points. As a result, fluid flow becomes dual, involving both petroleum and natural gas, with production favouring the lower-viscosity fluid, which is natural gas [7] (**Figure 1**).

An additional factor leading to an early bubble point is the pressure variation within the DFZ compared to other regions of the Uinta Basin. Hydrocarbon buildup caused over-pressurisation in a broad area directly north of the DFZ, which significantly contributed to fracturing the surrounding rocks throughout the basin [10,18]. Smith [10] noted that over-pressurisation was especially high north of the DFZ but decreased to normal levels once within the DFZ. If higher pressures trigger the initial surge in oil production north of the DFZ, then the relatively moderate pressures inside the DFZ may result in shorter production durations.

Without interconnected reservoirs and, to a lesser degree, lower pressures, vertical drilling becomes challenging in the heavily compartmentalised central DFZ. However, horizontal drilling addresses these issues. By extending laterally within a target zone, horizontal wells can access multiple isolated reservoirs and connect them through hydraulic fracturing. Longer wellbores enable the extraction from more compartmentalised reservoirs, greatly enhancing recovery and extending production lifespan. High-quality reservoir pressure data in different fault blocks within the fault zone were not available to us and were likely not collected, but we expect that blocks with better connectivity to the overpressured basin centre experienced better hydrocarbon charge and higher reservoir pressures. Blocks that are more effectively isolated by the fault zone have poorer charge characteristics and pressures.

5.2. Graben Width

Within the DFZ, the width of the grabens decreases from west to east. In the western area, older, wider, and more eroded rock units are exposed at the surface, as evidenced by the saline facies at the westernmost end of the DFZ. Moving eastward, this gradually transitions into the younger sandstone-limestone facies. Further to the east, the Member B facies of the younger Uinta Formation appears, characterised by clay-rich mudstone that is common in the eastern DFZ. Here, the grabens are notably narrower, as shown in **Figure 18**. The narrowing process begins only when transitioning into the Uinta Formation.

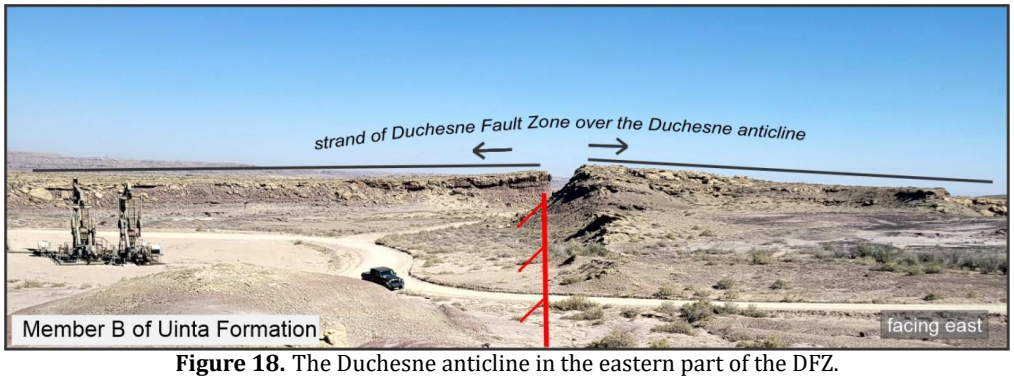

Figure 18. The Duchesne anticline in the eastern part of the DFZ.

Note: The black line shows the surface exposure of the anticline. There are no fractures due to the clay-rich mudstone, which is relatively ductile. The sediment originates from the Member B section of the Uinta Formation, dating back to the Eocene. The narrow graben displays north-south extension. See **Figure 2b** for the location.

Normal faults in this region occur within fractured sandstones containing oil seeps (**Figure 19**). Above these faulted sandstones, horse blocks appear, showing that large rock layers were pushed into the previously active DFZ. These horse blocks within the DFZ were dragged along the ridge of the Duchesne anticline. Although this might indicate strike-slip movement in the eastern DFZ, the presence of down-stepping plucking steps confirms that the faults here are mainly normal (**Figure 19**).

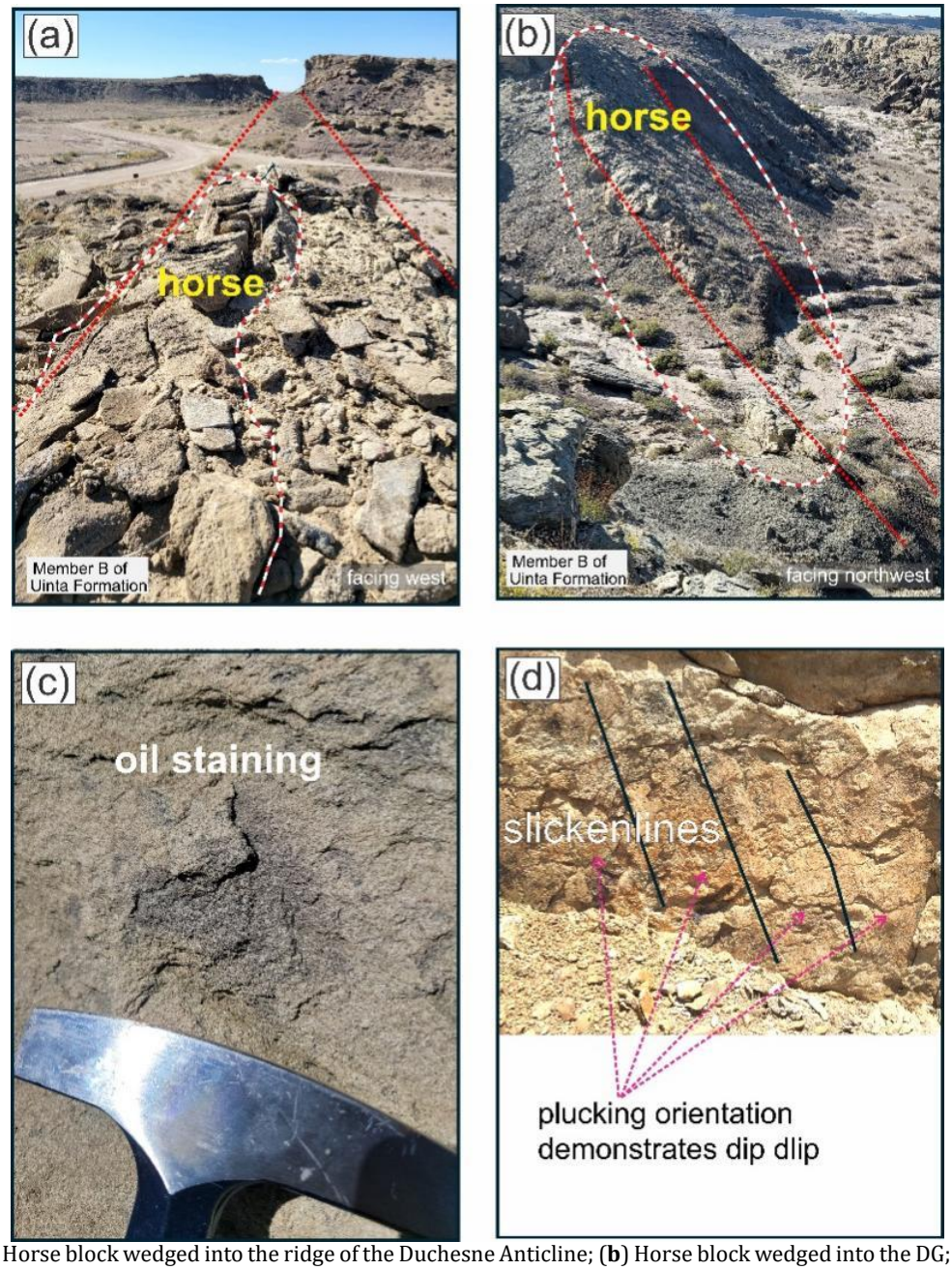

Figure 19. (**a**) Horse block wedged into the ridge of the Duchesne Anticline; (**b**) Horse block wedged into the DG; (**c**) Oil staining within sandstone of the Member B facies; (**d**) Down-stepping plucking steps on the foot wall of the DG in the eastern DG. See **Figure 2b** for the location.

The extensive oil staining in the eastern DFZ indicates the presence of petroleum reservoirs at depth. It implies that faulting within the DFZ has enhanced connectivity between these reservoirs and the Earth's surface (**Figure 16**). In the eastern DFZ, the compartmentalisation no longer exists.

5.3. Similarity to Other Eocene-Aged Fault Zones in the Uinta Basin

Within the Uinta Basin, several fault zones exhibit features similar to those we have observed in the DFZ: a large, open fold of lacustrine sediments with a zone of extension along the crest of the fold. The most extensively studied of these fault zones is the Sand Wash fault zone [8,43], owing to excellent exposures of this fault zone along cross-cutting canyon walls (**Figure 20**). This and other fault zones illustrated in **Figure 20** contain shallow grabens, with extension accommodated by slip on ductile oil shales, and the associated faults do not extend below or into these oil shales (Mahogany Oil Shale Zone, **Figure 4a**). Similar to the Duchesne fault zone, these faults cut the Green River Formation, appear to have been active during the Eocene, and are observable at the surface as long, straight traces across tens of miles. Both Brinkerhoff et al. [8] and Cardon [43] interpret the Sand Wash fault zone as resulting from Eocene-aged extension above a neutral surface, which aligns with the mechanism proposed here for the DFZ.

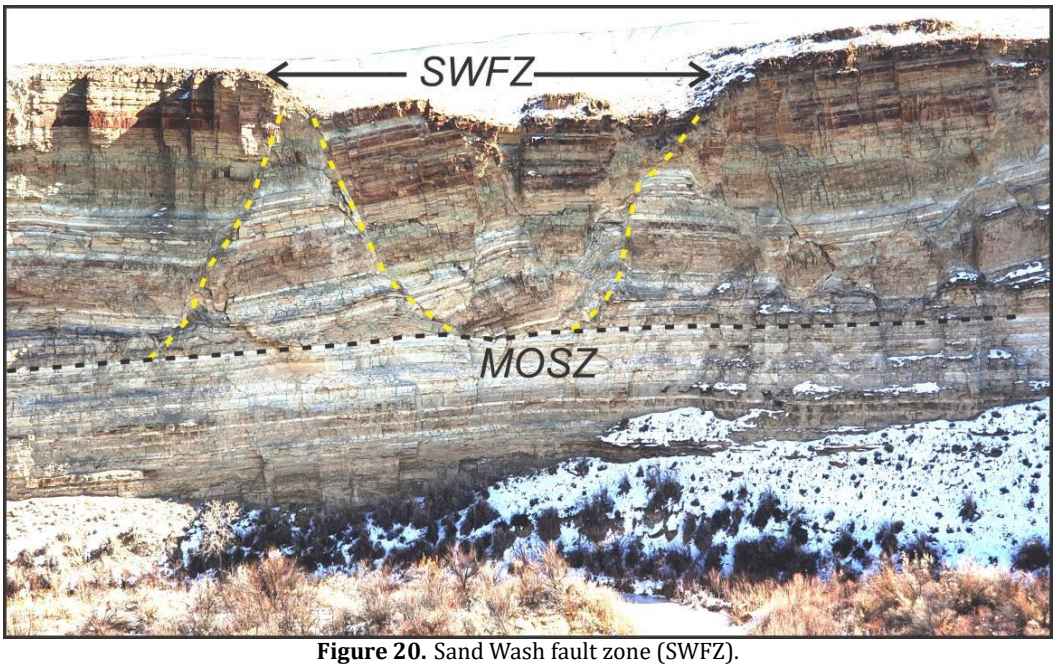

Figure 20. Sand Wash fault zone (SWFZ).
Note: MOSZ is the Mahogany Shale Zone, a series of highly ductile oil shales that accommodated slip on the fault zone. See **Figure 1** for the location. View is to the southeast, looking across Ninemile Canyon. Interpretation based on Cardon [43].
Source: Photo by J. McBride.

5.4. Limitations and the Need for Complementary Data

Historically, structural interpretations of the DFZ have heavily relied on aerial photography and surface geological mapping. While these traditional methods provide a foundation for delineating fault-surface traces and identifying large-scale geomorphological lineaments, they do not fully constrain the three-dimensional fault architecture. Relying solely on surface mapping introduces structural ambiguities, e.g., Quaternary sediment cover can obscure critical kinematic indicators and minor fault splays, potentially underestimating fault-zone complexity. Because outcrop data are essentially two-dimensional, they cannot definitively resolve variations in fault dip at depth or detect buried faults that do not rupture the modern topographic surface.

As subsurface datasets become more accessible, the uncertainties in surface mapping can start to be resolved. 2D and 3D seismic surveys offer continuous imaging of stratal geometries and fault surfaces at depth. This helps identify fault linkages, map vertical fault displacement, and interpret deep-crustal structural controls that lack surface expression. Our study utilises available petroleum exploration well-log data to characterise broad subsurface relationships associated with the DFZ. A more detailed, well-log-based analysis would

allow for precise correlation of stratigraphic horizons across the fault zone, quantify missing or repeated sections, and refine estimates of throw and heave.

6. Conclusions

We describe field and subsurface evidence of how the Duchesne Fault Zone (DFZ), a series of east-west trending *en echelon* faults in the Uinta Basin, developed synchronously above the neutral surface of the Duchesne Anticline during Laramide tectonism. Opposing stress regimes within the DFZ are indicated by our mapping of extensional and contractional structures. Thus, the DFZ acted as a hinge in the evolving Uinta Basin. Our findings provide structural evidence for the potential impact of compartmentalisation [44] within the DFZ. The combined stress from extensional forces above a neutral surface in the DG and reverse faulting linked to the Duchesne anticline has resulted in the segmentation of petroleum reservoirs in the Green River Formation. Faulting may also contribute to reservoir compartmentalization [33,45,46], as the tight compression along reverse faults forms barriers that restrict vertical permeability. Consequently, vertical drilling in the central DFZ is often unprofitable. Due to this structural setting, horizontal drilling [47] is recommended for hydrocarbon extraction, particularly in the central region. The widespread fracturing throughout the DFZ creates natural pathways for fluid movement, which can be exploited during production. Furthermore, horizontal drilling can intersect multiple segmented reservoirs, enhance connectivity, and increase productivity.

Author Contributions

Conceptualization, A.R.B., A.K. and J.M.; methodology, A.K., R.A.H. and K.A.R.; software, S.M.H.; validation, A.K., R.A.H., A.R.B., S.M.H. and J.M.; formal analysis, A.K. and R.A.H.; investigation, A.R.B., A.K. and J.M.; resources, J.M. and K.A.R.; data curation, J.M.; writing—original draft preparation, A.K. and J.M.; writing—review and editing, J.M., A.R.B., R.A.H. and S.M.H.; visualization, A.K. and A.R.B.; supervision, J.M., S.M.H. and R.A.H.; project administration, J.M.; funding acquisition, J.M. All authors have read and agreed to the published version of the manuscript.

Funding

The Brigham Young University College of Computational, Mathematical, and Physical Sciences graciously provided funding for this project.

Institutional Review Board Statement

Not applicable.

Informed Consent Statement

Not applicable.

Data Availability Statement

Data associated with this project may be requested from the corresponding author.

Acknowledgments

The authors gratefully acknowledge the referees, whose comments, recommendations, and corrections greatly improved the final version of the paper.

Conflicts of Interest

The authors declare no conflict of interest.

References

[1] Sprinkel, D.A., 2024. Geologic Map of the Duchesne 30′ × 60′ Quadrangle, Duchesne and Wasatch Counties, Utah, Scale 1:100,000. Utah Geological Survey: Salt Lake City, UT, USA. Available from: https://ugspub.nr.utah.gov/publications/maps/m-300/m-300.pdf

[2] Black, B.D., Hecker, S., 1999. Fault Number 2414, Duchesne-Pleasant Valley Fault System. In Quaternary Fault and Fold Database of the United States. United States Geological Survey: Reston, VA, USA. Available from: https://earthquake.usgs.gov/static/lfs/nshm/qfaults/Reports/2414.pdf

[3] Groeger, A., Bruhn, R., 2001. Structure and geomorphology of the Duchesne graben, Uinta basin, Utah,

and its enhancement of a hydrocarbon reservoir. AAPG Bulletin. 85. DOI: https://doi.org/10.1306/8626CCF3-173B-11D7-8645000102C1865D

[4] Brinkerhoff, R., Sprinkel, D.A., 2021. Structural Geometry, Kinematics, and Timing of the Duchesne Fault Zone, Uinta Basin, Northeastern Utah, USA. In Proceedings of the 2021 International Meeting for Applied Geoscience & Energy, Denver, CO, USA, 26 September–1 October 2021. DOI: https://doi.org/10.1306/11368Brinkerhoff2022

[5] Martin, R.A., Nelson, A.R., Weisser, R.R., et al., 1985. Seismotectonic Study for Taskeech Dam and Reservoir Site, Upalco Unit and Upper Stillwater Dam and Reservoir Site, Bonneville Unit, Central Utah Project, Utah. Bureau of Reclamation Seismotectonic: Denver, CO, U.S.A. Available from: https://ugspub.nr.utah.gov/publications/misc_pubs/mp11-02/85-2.pdf

[6] Utah Geological Survey. Characteristics of the Duchesne Fault Zone. Available from: https://geology.utah.gov/docs/emp/greenriver/poster02/poster2.pdf (cited 1 January 2026).

[7] Brinkerhoff, R., Sprinkel, D.A., 2021. The Duchesne Fault Zone's Impact on Horizontal Development Within the Burgeoning Green River Oil Play, Uinta Basin, Northeastern Utah, USA. In Proceedings of the 2021 International Meeting for Applied Geoscience & Energy, Denver, CO, USA, 26 September–1 October 2021. DOI: https://doi.org/10.1306/11367Brinkerhoff2022

[8] Brinkerhoff, R., McBride, J., Hudson, S., et al., 2022. Strain Segregation between Ductile and Brittle Stratigraphy —Characterizing the Sand Wash Fault System, Uinta Basin, Utah. In Proceedings of the 2022 AAPG Rocky Mountain Section Meeting, Denver, CO, USA, 24–27 July 2022. DOI: https://doi.org/10.1306/11363Brinkerhoff2022

[9] Brinkerhoff, R., Sprinkel, D.A., 2021. The Duchesne Fault Zone and its impact on the development of the Uinta Basin. OUTCROP. 70(3), 16–20.

[10] Smith, J.L., 2004. Investigation of Fracture Mechanisms in the Duchesne Fault Zone, Uinta Basin, Northeastern Utah: The Role of Fluid Overpressures and Other Processes [Master's Thesis]. New Mexico Institute of Mining and Technology: Socorro, NM, USA. Available from: https://www.nmt.edu/academics/ees/theses/theses_1936-2014/2004t_smith_jl.pdf

[11] Osborn, G.D., 1973. Quaternary Geology and Geomorphology of the Uinta Basin and the South Flank of the Uinta Mountains, Utah [PhD Thesis]. University of California: Berkeley, CA, USA.

[12] Sullivan, J.T., 1988. Late Cenozoic Uplift of the Uinta Mountains and Inversion of the Uinta Basin. In Geology of the Uinta Mountains. Utah Geological Association Publication: Salt Lake City, UT, USA.

[13] Raschilla, R.N., 2013. Hydrocarbon Potential of the Upper Green River Petroleum System in the Uinta Basin, Utah: A Basin Modeling Approach [Master's Thesis]. University of Houston: Houston, TX, USA. Available from: http://hdl.handle.net/10657/969 (cited 27 February 2026).

[14] Brinkerhoff, R., Vanden Berg, M., Millard, M., 2022. Using Pore System Characterization to Subdivide the Burgeoning Uteland Butte Play, Green River Formation, Uinta Basin, Utah. In Proceedings of the 2022 AAPG Rocky Mountain Section Meeting, Denver, CO, USA, 24–27 July 2022. DOI: https://doi.org/10.1306/11364Brinkerhoff2022

[15] Morgan, C.D., Gwynn, J.W., Allison, M.L., et al., 2003. The Bluebell Oil Field, Uinta Basin, Duchesne and Uintah Counties, Utah: Characterization and Oil Well Demonstration. Utah Geological Survey: Salt Lake City, UT, USA. Available from: https://ugspub.nr.utah.gov/publications/special_studies/SS-106.pdf

[16] Morgan, C.D., McClure, K.P., Bereskin, S.R., et al., 2002. A Preliminary Discussion of Fault Styles in the Southwest Uinta Basin, Utah. Available from: https://www.searchanddiscovery.com/abstracts/html/2002/rms/images/morgan01.htm (cited 1 January 2026).

[17] Johnson, R.C., 2003. Northwest to southeast cross section of Cretaceous and Lower Tertiary rocks across the eastern part of the Uinta Basin, Utah. In Petroleum Systems and Geologic Assessment of Oil and Gas in the Uinta-Piceance Province, Utah and Colorado. U.S. Geological Survey: Denver, CO, USA. Available from: https://pubs.usgs.gov/dds/dds-069/dds-069-b/REPORTS/Chapter_11.pdf

[18] Washburn, A.M., Sylvester, P.J., Snell, K.E., 2025. Deep Basin Overpressure Resulting From Fluid Migration and Hydraulic Head in the Uinta Basin: Insights From Beef Calcite in the Green River Formation. Basin Research. 37(4), e70052. DOI: https://doi.org/10.1111/bre.70052

[19] Verbeek, E.R., Grout, M.A., 1993. Geometry and structural evolution of gilsonite dikes in the eastern Uinta Basin, Utah. U.S. Geological Survey Bulletin. 1787. DOI: https://doi.org/10.3133/b1787HH

[20] Boden, T., Tripp, B.T., 2012. Gilsonite Veins of the Uinta Basin, Utah. Utah Geological Survey: Salt Lake City, UT, USA. Available from: https://ugspub.nr.utah.gov/publications/special_studies/ss-141.pdf

[21] USGS Quaternary Fault and Fold Database, Fault number 2414, Duchesne fault zone. Available from: https://earthquake.usgs.gov/static/lfs/nshm/qfaults/Reports/2414.pdf (cited 1 January 2026).

[22] Jensen, M., Kowallis, B., Christiansen, E., et al., 2020. Fallout tuffs in the Eocene Duchesne River Formation, northeastern Utah—Ages, compositions, and likely source. Geology of the Intermountain West. 7, 1–27. DOI: https://doi.org/10.31711/giw.v7.pp1-27

[23] Bryant, B., Naeser, C.W., Marvin, R.F., et al., 1989. Upper Cretaceous and Paleogene sedimentary rocks and isotopic ages of Paleogene tuffs, Uinta basin, Utah. Ages of late Paleogene and Neogene tuffs and the beginning of rapid regional extension, eastern boundary of the Basin and Range Province near Salt Lake City, Utah. U.S. Geological Survey Bulletin. 1787. DOI: https://doi.org/10.3133/b1787JK

[24] Kowallis, B., Christiansen, E., Balls, E., et al., 2005. The Bishop Conglomerate ash beds, south flank of the Uinta Mountains, Utah: Are they pyroclastic fall beds from the Oligocene ignimbrites of western Utah and eastern Nevada? Utah Geological Association Publication. 33, 131–145.

[25] Gearon, J.H., Olariu, C., Steel, R.J., 2022. The supply-generated sequence: A unified sequence-stratigraphic model for closed lacustrine sedimentary basins with evidence from the Green River Formation, Uinta Basin, Utah, U.S.A. Journal of Sedimentary Research. 92(9), 813–835. DOI: https://doi.org/10.2110/jsr.2021.096

[26] DeCelles, P.G., 2004. Late Jurassic to Eocene evolution of the Cordilleran thrust belt and foreland basin system, western U.S.A. American Journal of Science. 304(2), 105–168. DOI: https://doi.org/10.2475/ajs.304.2.105

[27] Anderson, D.W., Picard, M.D., 1972. Stratigraphy of the Duchesne River formation (Eocene-Oligocene?) Northern Uinta Basin, Northeastern Utah. Bulletin of Utah Geological and Mineralogical Survey. 97, 1–29.

[28] Bryant, B., Naeser, C.W., Marvin, R.F., et al., 1989. Ages of Late Paleogene and Neogene Tuffs and the Beginning of Rapid Regional Extension, Eastern Boundary of the Basin and Range Province Near Salt Lake City, Utah. United States Geological Survey: Reston, VA, USA.

[29] Smith, R.B., Sbar, M.L., 1974. Contemporary Tectonics and Seismicity of the Western United States with Emphasis on the Intermountain Seismic Belt. Geological Society of America Bulletin. 85(8), 1205. DOI: https://doi.org/10.1130/0016-7606(1974)85%253C1205:CTASOT%253E2.0.CO;2

[30] Mayr, G., Weidig, I., 2004. The Early Eocene bird Gallinuloides wyomingensis—A stem group representative of Galliformes. Acta Palaeontologica Polonica. 49(2), 211–217. Available from: https://app.pan.pl/archive/published/app49/app49-211.pdf

[31] Nel, A., Garrouste, R., Engel, M.S., 2023. The earliest Pupipara (Diptera: Hippoboscoidea): A new genus and species from the lower Eocene of the Green River Formation. Palaeoentomology. 6(1). DOI: https://doi.org/10.11646/palaeoentomology.6.1.9

[32] Rasmussen, D.T., Conroy, G.C., Friscia, A.R., et al., 1999. Mammals of the Middle Eocene Uinta Formation. In Fossil Vertebrates of Utah. Utah Geological Survey: Salt Lake City UT, USA. pp. 401–420.

[33] Ejeke, C.F., Anakwuba, E.E., Preye, I.T., et al., 2017. Evaluation of reservoir compartmentalization and property trends using static modelling and sequence stratigraphy. Journal of Petroleum Exploration and Production Technology. 7(2), 361–377. DOI: https://doi.org/10.1007/s13202-016-0285-z

[34] Schmude, D., Berwick, B., 1969. Lacustrine source rocks and unconventional oil resource plays: A case study from the Eocene Green River Formation of the Uinta Basin, Utah. Geosites. 50, 1–25. DOI: https://doi.org/10.31711/ugap.v50i.107

[35] Chidsey, T.C., Allison, M.L., Morgan, C.D., 2003. Major Oil Plays in Utah and Vicinity. Utah Geological Survey: Salt Lake City, UT, USA. Available from: https://geology.utah.gov/docs/emp/pump/pdf/pumprpt14.pdf

[36] Ramsay, J.G., 1967. Folding and Fracturing of Rocks. McGraw-Hill: New York, NY, USA.

[37] Turcotte, D.L., Schubert, G., 2002. Geodynamics, 2nd ed. Cambridge University Press: Cambridge, UK. DOI: https://doi.org/10.1017/CBO9780511807442

[38] Price, N.J., Cosgrove, J.W., 1990. Analysis of Geological Structures. Cambridge University Press: Cambridge, UK.

[39] Lisle, R.J., Aller, J., Bastida, F., et al., 2009. Volumetric strains in neutral surface folding. Terra Nova. 21(1), 14–20. DOI: https://doi.org/10.1111/j.1365-3121.2008.00846.x

[40] Bobillo-Ares, N.C., Aller, J., Bastida, F., et al., 2006. The problem of area change in tangential longitudinal strain folding. Journal of Structural Geology. 28(10), 1835–1848. DOI: https://doi.org/10.1016/j.jsg.2006.07.004

[41] Schultz, R.A., 2019. Deformation Bands: In Geologic Fracture Mechanics. Cambridge University Press: Cambridge, UK.

[42] Ketring, A.M., 2025. Influence of the Duchesne Fault Zone on Oil Production in the Uinta Basin[Master's Thesis]. Brigham Young University: Provo, UT, USA. Available from: https://scholarsarchive.byu.edu/etd/10811

[43] Cardon, B.L., 2024. Geological and Geophysical Model of the Sand Wash Extensional Decolle-

ment [Master's Thesis]. Brigham Young University: Provo, UT, USA. Available from: https://scholarsarchive.byu.edu/etd/10543

[44] Morris, A.P., Smart, K., Ferrill, D.A., et al., 2012. Fault compartmentalization in a mature clastic reservoir: An example from Elk Hills Field, California. Available from: https://www.searchanddiscovery.com/pdfz/documents/2012/40907morris/ndx_morris.pdf.html (cited 23 June 2025).

[45] Hui, G., Chen, Z., Schultz, R., et al., 2023. Intricate unconventional fracture networks provide fluid diffusion pathways to reactivate pre-existing faults in unconventional reservoirs. Energy. 282, 128803. DOI: https://doi.org/10.1016/j.energy.2023.128803

[46] Asemani, M., Kouhanjani, M.H.S., Rabbani, A.R., 2025. Developing a straightforward and robust approach for investigating reservoir compartmentalization based on chemical composition heterogeneities. Scientific Reports. 15(1), 44342. DOI: https://doi.org/10.1038/s41598-025-27994-8

[47] Maxwell, S., Ritter, G., Tuttle, T., et al., 2024. Analysis of Zonal Interference through Integrated Stimulation and Drainage Diagnostic Measurements in the Uinta Basin, Utah, USA: Microseismic, Crosswell Strain, Offset Pressure Fracture Measurement, and Geochemical Fingerprinting of Produced Hydrocarbons. In Proceedings of the Unconventional Resources Technology Conference, Houston, TX, USA, 17–19 June 2024. DOI: https://doi.org/10.15530/urtec-2024-4043150